EXPLORATORY RESEARCH

sesar JOINT UNDERTAKING

FlyATM4E D1.2 – Report on expanded aCCFs including robustness and eco-efficiency aspect

Deliverable ID:	**D1.2**
Dissemination Level:	**PU**
Project Acronym:	**FlyATM4E**
Grant:	**891317**
Call:	**Call: H2020-SESAR-2019-2**
Topic:	**ER4 (H2020-2019-2)**
Consortium Coordinator:	**DLR**
Edition date:	**21 November 2022**
Edition:	**00.04.00**
Template Edition:	**02.00.05**

EUROPEAN PARTNERSHIP

Co-funded by the European Union

Authoring & Approval

Name / Beneficiary	Position / Title	Date
Simone Dietmüller (DLR)	Project member	20/06/2022
Sigrun Matthes (DLR)	Coordinator/WP1 Leader	20/06/2022

Reviewers internal to the project

Name / Beneficiary	Position / Title	Date
Feijia Yin (TU Delft)	WP3 leader	23/06/2022
Baumann Sabine (DLR)	Deputy coordinator	13/09/2022

Approved for submission to the SJU By - Representatives of all beneficiaries involved in the project

Name / Beneficiary	Position / Title	Date
Sigrun Matthes (DLR)	Coordinator/WP1 Leader	13/09/2022
Feijia Yin (TU Delft)	WP3 Leader	05/06/2022
Manuel Soler (UC3M)	WP4 Leader	05/07/2022
Sabine Baumann (DLR)	Deputy Coordinator	13/09/2022
Maximilian M. Meuser (TUHH)	WP2 contributor	05/07/2022

Document History

Edition	Date	Status	Name / Beneficiary	Justification
00.00.01	30/05/2022	Initial Draft	Simone Dietmüller(DLR)	New document
00.00.02	20/06/2022	Complete Draft	Simone Dietmüller(DLR)	internal review
00.00.10	23/06/2022	Reviewed Draft	Simone Dietmüller(DLR)	Reviewed document
00.00.12	08/07/2022	Complete Report	Simone Dietmüller(DLR)	Internal review
00.01.00	08/07/2022	Submitted Report	Simone Dietmüller(DLR)	Final version
00.01.01	16/08/2022	Updated Report	Simone Dietmüller(DLR)	Updated document
00.02.00	24/08/2022	Submitted Report	Simone Dietmüller(DLR)	Submitted document
00.02.01	12/09/2022	Updated Report	Simone Dietmüller(DLR)	Updated document
00.03.00	13/09/2022	Submitted Report	Simone Dietmüller(DLR)	Submitted document
00.04.00	21/11/2022	Submitted Report	Simone Dietmüller(DLR)	Submitted document

Copyright Statement

FlyATM4E

FLYING AIR TRAFFIC MANAGEMENT FOR THE BENEFIT OF ENVIRONMENT AND CLIMATE

This Deliverable is part of a project that has received funding from the SESAR Joint Undertaking under grant agreement No 891317 under European Union's Horizon 2020 research and innovation programme.

Abstract

The objective of this Deliverable is to provide a description of the expanded prototype algorithmic climate change functions (aCCFs), which have been applied in the overall FlyATM4E multi-modelling concept in order to explore the mitigation potential of climate optimized aircraft trajectories (i.e. FlyATM4E work package WP2 and WP3).

Algorithmic climate change functions (aCCFs) represent spatially and temporally resolved information on the climate effects in terms of future temperature changes resulting from aviation emissions at a given time and location in the atmosphere. They include CO_2 and non-CO_2 effects, comprising NO_x, water vapour and contrail-cirrus. These aCCFs can be simply derived from meteorological weather forecast data. As these aCCFs are the object of uncertainties from weather forecasts and climate science, the described aCCFs also include robustness aspects. For this purpose, a novel concept has been developed on exploring climate-optimization of aircraft trajectories and the robustness of estimated benefits in terms of mitigation of climate effects. This is done by a systematic risk analysis relying on a Monte-Carlo Method.

Further, it is shown that by combining the individual aCCFs of water vapour, NO_x and contrail-cirrus, merged non-CO_2 aCCFs can be generated. Technically this is done with an open-source Python Library. Both individual and merged aCCF patterns were analysed and show the dominating effect of the contrail aCCF in areas where contrails are forming. Further analysing the variability in aCCFs reveals a clear seasonal cycle in NO_x and contrail aCCFs and a strong variability with different synoptical weather situations and cruise altitudes.

Results presented in this deliverable contribute to the overall project objective O1, which is to advance concepts to assess the climate impact of ATM operations while integrating an adequate representation of uncertainties, including CO_2, contrails, ozone, methane, and water vapour climate effects, from weather forecast as well as climate science, and provide concepts for climate information enabling eco-efficient aircraft trajectories.

EUROPEAN PARTNERSHIP

Co-funded by the European Union

Table of Contents

Abstract 3
1 Introduction 7
1.1 Background 7
1.2 Purpose 7
2 Algorithmic climate change functions and the characterization of their uncertainties . 9
2.1 Climate impact of aviation 9
2.2 Prototype Algorithmic climate change functions 10
2.3 Enhanced aCCFs – Development of educated guess aCCFs 10
2.4 Characterisation of uncertainties in aCCFs 11
2.5 Concept towards robust aCCFs by integrating uncertainties 14
3 Generating merged aCCFs 18
3.1 Concept of generating merged aCCFs 18
3.2 Choice of emission index 18
3.3 Choice of climate metric and efficacy 20
3.4 Technical implementation of individual and merged aCCFs using a Python Library 21
4 Systematic analysis of individual aCCF patterns 24
4.1 Description of calculated aCCFs 24
4.2 Characteristic aCCF patterns of specific winter and summer days 24
4.3 Variation of aCCFs with season 26
4.4 Variation of aCCFs with cruise altitude 27
4.5 aCCFs calculated from EPS weather forecast 28
4.6 Guidance on and analysis of situations with high mitigation potential 29
5 Sensitivity of merged aCCFs to aircraft type 31
5.1 Description of merged aCCF calculations 31
5.2 Analysis of aircraft-engine dependent merged aCCFs 31
6 Summary and Conclusion 33
7 References 35
Appendix A Mathematical formulation of aCCFs 38
A.1 NO_x induced aCCFs 38
A.2 Ozone aCCFs 38

EUROPEAN PARTNERSHIP

Co-funded by the European Union

A.3 Methane aCCFs 38
A.4 Water vapour aCCFs 39
A.5 Contrail aCCFs 39
A.6 CO_2 aCCF 40
Appendix B Additional figures 41
B.1 Synoptic situation for selected days 41
B.2 Weather pattern classification 43
B.3 Analysis of night time aCCFs 44
B.4 Vertical profile of aCCFs 46
Acronyms and FlyATM4E consortium 47

List of Tables

Table 1: List of sources of uncertainties for individual aCCFs and for their associated calculations on climate effect 12

Table 2: Uncertainty ranges for the individual species given for different sources of uncertainties and different forcing species. For the radiative forcing (RF) and the climate sensitivity parameter (λ), the median, the upper and lower limit of the 95% likelihood is given together with the underlying distributions. Estimates are based on [1] [20]. 17

Table 3: Average specific NOx emission indices (in g(NO2)) for three aircraft classes (regional, single-aisle, widebody) derived from the emission inventory of the DLR project "Transport and Climate" (TraK). EINOx are shown for various typical flight altitudes (20000 ft - 40000 ft). Besides the flight altitude in ft, the corresponding pressure level is given in hPa. Table taken from submitted publication [10]. 19

Table 4: Average flown distance per burnt fuel(km/kg(fuel)) for three aircraft classes (regional, single-sisle, widebody) derived from the TraK emission inventory. EINOx is shown for various typical flight altitudes (20000 ft - 40000 ft). Besides the flight altitude in ft, the corresponding pressure level is given in hPa. Table taken from submitted publication [10]. 19

Table 5: Climate metric conversion factors from P-ATR20 (pulse emission over time horizon of 20 years) to F-ATR20 (increasing future emission scenario over time horizon of 20 years), F-ATR50 (increasing future emission scenario over time horizon of 50 years), and F-ATR100 (increasing future emission scenario over time horizon of 100 years), for water vapour, ozone, methane, PMO, contrail cirrus and CO_2 aCCFs. Table taken from submitted publication [10]. 20

Table 6: Overview of state-of-the-art efficacies of NO_x induced ozone, methane, primary mode ozone (PMO), as well as water vapour and contrails. Respective references are given in the right side of the table. 21

Table 7: Meteorological input parameter to calculate aCCFs within CLIMaCCF 22

Table 8: Overview of calculated merged non-CO_2 aCCF. Four technical specification of aircraft-engine type selection are possible. 31

EUROPEAN PARTNERSHIP
Co-funded by the European Union

Table 9: Non-exhaustive list of acronyms used across the text. 47

Table 10: FlyATM4E consortium acronyms 48

List of Figures

Figure 1: Effective radiative forcing from the individual emissions of global aviation for the years 1940-2018. Best estimates and their confidence intervals (showing the 5% and the 95% percentiles) are given. Red bars indicate warming impact and blue bars cooling impact This figure is taken from [1] .. 9

Figure 2 Schematic workflow of calculating merged aCCFs using the Python Library CLIMaCCF. The left row describes the Input block, the top raw the processing block and the bottom raw the output block. 22

Figure 3 . Characteristic patterns of (a) water vapour aCCF [K/kg($_{fuel}$)] (b) NO_x aCCF (including O_3, CH_4 and PMO) [K/kg(fuel)] (c) contrail (daytime) aCCF [K/kg(fuel)] (d) merged non-CO_2 aCCF [K/kg(fuel)] at pressure level 250 hPa over European region for 5 selected days in June 2018, at 12UTC. Individual aCCFs were calculated from ERA5 reanalysis data. Overlaid green lines indicate wind speeds over 30 m/s$^{2.}$ Moreover, the weather situation of the specific days was classified according to [27] and is given right beside the date. 26

Figure 4 . Characteristic patterns of aCCF (a) water vapour aCCF [K/kg($_{fuel}$)] (b) NO_x aCCF (including O_3, CH_4 and PMO) [K/kg(fuel)] (c) contrail (daytime) aCCF [K/kg(fuel)] (d) merged non-CO_2 aCCF [K/kg(fuel)] at pressure level 250 hPa over European region for 5 selected days in December 2018, at 12UTC. Individual aCCFs were calculated from ERA5 reanalysis data. Overlaid green lines indicate wind speeds over 30 m/s$^{2.}$ Moreover, the weather situation of the specific days was classified according [27] and is given right beside the date..... 27

Figure 5 . Vertical cross section patterns of aCCF (a) water vapour aCCF [K/kg($_{fuel}$)] (b) NO_x aCCF (including O_3, CH_4 and PMO) [K/kg(fuel)] (c) contrail (daytime) aCCF [K/kg(fuel)] (d) merged non-CO_2 aCCF [K/kg(fuel)] at longitude 0° for 5 selected days in June 2018, at 12UTC. Individual aCCFs were calculated from ERA5 reanalysis data. 28

Figure 6 . Characteristic patterns of the ensemble mean (a) NO_x aCCF [K/kg($_{fuel}$)] and (b) contrail (daytime) aCCF [K/kg(fuel)]. The corresponding standard deviations are given for (c) NO_x aCCF and (d) contrail aCCF. All figures are displayed at pressure level 250 hPa over European region on 13th June 2018, 12UTC. aCCFs were calculated from 50 ensemble members of an EPS weather forecast. 29

Figure 7 . Characteristic patterns of (a) water vapour aCCF [K/kg($_{fuel}$)] (b) NO_xaCCF (including O_3, CH_4 and PMO) [K/kg(fuel)] (c) contrail (daytime) aCCF [K/kg(fuel)] (d) merged non-CO_2 aCCF [K/kg(fuel)] at pressure level 250 hPa over European region for 15th of June 2018 (12 UTC). Individual and merged non-CO_2 aCCF are shown for four different assumptions for the NO_x emission index and flown km. For typical transatlantic fleet mean (first raw) Regional aircraft type (second raw), single aisle aircraft type (third raw) and widebody aircraft type values (forth raw). 32

EUROPEAN PARTNERSHIP

Co-funded by the European Union

1 Introduction

1.1 Background

The overall objective of the project FlyATM4E is to develop a concept to identify climate-optimised aircraft trajectories in which Air Traffic Management (ATM) can help to provide a robust and eco-efficient reduction in aviation's climate impact and to estimate the mitigation potential. The project considers carbon dioxide (CO_2) and non-CO_2 emissions through meteorological (MET) data, ensemble prediction and eco-efficient trajectories. So-called algorithmic climate change functions (aCCFs) enable to assess aviation's climate impact for trajectory optimisation at a particular time and geographical location and cover both the global CO_2 and non-CO_2 effects. The non-CO_2 effects considered within FlyATM4E comprise the impact of nitrogen oxide (NO_x) emissions on both ozone and methane, of water vapour, and of contrail-cirrus.

The main goal of work package 1 (WP1) is to advance concepts to assess the climate impact of ATM operations which integrates an adequate representation of uncertainties, including CO_2, contrails, ozone, methane and water vapour climate effects, from weather forecast as well as climate science, and to provide concepts for climate information enabling eco-efficient aircraft trajectories.

The specific research goals of the FlyATM4E WP1 are:

- to enhance the algorithmic climate change functions by providing spatially and temporally resolved quantitative information on the climate impact of individual aviation emissions.
- to incorporate uncertainties of aCCFs arising from atmospheric variability, limited predictabilities and low level of scientific understanding from atmospheric modelling, by using the Ensemble Prediction System (EPS) weather forecast through the development of concepts, which integrates information on uncertainties based on a systematic assessment of specific sources of uncertainty.
- to integrate information on robustness which can support the identification of favourable situations such as win-win and eco-efficient situations into revised aCCFs leading to robust aCCFs.

1.2 Purpose

The main goal of this deliverable is to provide a description of the expanded algorithmic climate change functions, which are made available for the overall FlyATM4E modelling chain of climate-optimisation of aircraft trajectories. They are a key element of the solution Sol-FlyATM4E-01. These expanded aCCFs respond to additional requirements and enhancements while including both robustness and eco-efficiency aspects.

After a brief introduction to mechanisms and processes of climate impact of global aviation (Section 2.1), the algorithmic climate change functions, which provide the spatial and temporal information on the climate impact of individual aviation emissions, are described (Section 2.2). A detailed characterization of the uncertainties in individual aCCFs arising from low level understanding of climate science and meteorological forecast follows in Section 2.3. This characterization includes the identification of the different sources of uncertainties and also the quantification of these uncertainties according to the recent state of the art research. The advancing concept of assessing the climate impact of ATM operations, which integrates an adequate representation of uncertainties, is

EUROPEAN PARTNERSHIP
Co-funded by the European Union

then explained (Section 2.4.). Section 3 informs on the underlying concept and the technical implementation of how to generate merged non-CO_2 aCCFs. These merged aCCFs combine the individual non-CO_2 algorithmic climate change functions by using technical specifications, e.g. engine-aircraft dependent emission indices and climate metrics. Various analyses of the spatially and temporally resolved individual and merged aCCFs are presented in Section 4, by showing their characteristic patterns for several specific days (selected in WP2). Also, preferable areas are characterized by a large potential for mitigation of climate effects by reducing non-CO_2 effects, as well as those regions where analysis of win-win solutions is expected to be favourable. Moreover, in Section 5, the sensitivity of merged aCCF to different specific technical specifications is identified from selected engine-aircraft combinations and from selected climate metrics. A summary and conclusion follow in Section 6.

EUROPEAN PARTNERSHIP

Co-funded by the European Union

2 Algorithmic climate change functions and the characterization of their uncertainties

2.1 Climate impact of aviation

Global aviation emissions contribute to anthropogenic climate change by warming the Earth's near-surface atmosphere through carbon dioxide (CO_2) and non-CO_2 emissions [1]. Non-CO_2 emissions comprise mainly water vapour (H_2O), nitrogen oxide (NO_x), sulphur oxides and soot. Not all non-CO_2 emissions have a direct effect on climate. Thus e.g. NO_x emissions are not radiatively active themselves, but they are responsible for the chemical production of the greenhouse gas (GHG) ozone (O_3) and the destruction of the GHG methane (CH_4). Furthermore, induced by non-CO_2 emissions, contrails and contrail-cirrus can form and alter the radiation budget (radiative forcing RF). Figure 1, which is taken from [1], provides state-of-the-art estimates and their uncertainties (by showing the 5% and the 95% percentiles) of the global aviation climate impact for individual forcing components. These estimates are given in effective radiative forcing (ERF) in mWm^{-2}. The ERF is a very useful definition as it includes instantaneous radiative flux change and the rapid adjustment of the atmosphere induced by a certain perturbation. Red bars indicate warming, while blue bars indicate a cooling of the atmosphere. Comparing the individual forcing components in Figure 1 reveals that the largest contributions to the overall positive effective radiative forcing are due to CO_2, H_2O, and net NO_x emissions as well as due to contrail-cirrus formation. Overall, the non-CO_2 emissions are responsible for roughly 2/3 of aviation's global net effective radiative forcing [1]. In contrast to CO_2, which is a long-living and well-mixed GHG, the climate impact of non-CO_2 effects depends, besides the quantity of emission, on the altitude, geographical location, and time of the emission [1] [4].

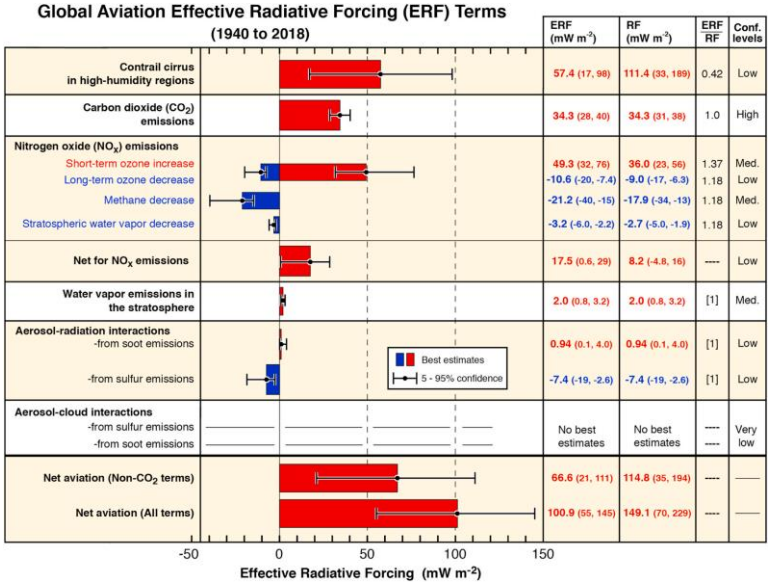

Figure 1: Effective radiative forcing from the individual emissions of global aviation for the years 1940-2018. Best estimates and their confidence intervals (showing the 5% and the 95% percentiles) are given. Red bars indicate warming impact and blue bars cooling impact This figure is taken from [1]

EUROPEAN PARTNERSHIP

Co-funded by the European Union

2.2 Prototype Algorithmic climate change functions

In order to enable climate optimization of aircraft trajectories during the trajectory planning process, it is required to have available spatially and temporally resolved information on the total climate effect of aviation emissions – comprising CO_2 and non-CO_2 effects – for the entire airspace or a dedicated planning domain, e.g., the flight corridor where the aircraft is flying. To be able to quantify the climate effects of non-CO_2 emissions at a specific location and time, the concept of the climate-change functions (CCFs) was developed [1][4], which derive such information from comprehensive chemistry-climate numerical simulations. These CCFs provide a measure of the climate impact of a given emission by using the average temperature response over the future time period of 20 years (ATR20). In the EU project REACT4C, these CCFs were calculated in climate model simulations for NO_x and H_2O emissions and persistent contrail-cirrus over the North-Atlantic region for eight specific days [1]. Note that for these eight days, representative weather types in summer and winter were considered. As the calculation of these CCFs is computationally very demanding, it cannot be used operationally for trajectory optimization.

An efficient implementation concept has been proposed which was using statistical methods relying on correlation in order to derive algorithms by linking these CCFs calculated in climate model simulations to the corresponding local meteorological data for selected meteorological parameters, e.g., temperature or geopotential height [3]. These algorithms (mathematical formulas) calculate the climate effect of non-CO_2 and CO_2 effects of aviation while depending on atmospheric parameters in the dedicated meteorological situation and produce the algorithmic climate change functions (aCCFs). The strength of these generated aCCFs is that they are an efficient tool for implementation in daily flight planning as their mathematical formulation only requires on relevant local weather data (e.g. meteorological data fields from numerical weather prediction for a specific day). Thus, they could be directly implemented in numerical weather prediction models in order to output such an advanced MET info which can then be used by the airspace users for flight planning. Note that the aCCF are calculated by using input data from numerical weather prediction data at individual timesteps. Hence the temporal (and spatial) resolution of aCCFs if determined by the resolution of the integrated numerical weather prediction data. Currently flight planning uses time resolution of up to hour, which is expected to represent high temporal variability in contrail formation to a certain degree. Using a resolution which is too coarse would result in lower efficiency of mitigation, as the information available during the flight planning would not be correct compared to the real situation encountered by the aircraft. Here, to our experience a time resolution of 6 hours would not be enough for using aCCFs for flight planning. An initial detailed description of these aCCFs has been given in Deliverable D1.1 [12], and an updated consistent set of prototype aCCF formulations is given in a scientific publication [8].

The development of the current aCCFs relied on comprehensive simulations with a climate chemistry model for Lagrangian trajectories departing from the North Atlantic flight corridor (NAFC) during summer and winter months, which were investigated in a set of archetypical synoptic situations. These are constructed with the help of atmospheric indices (North Atlantic Oscillation and Atlantic Oscillation) to represent atmospheric variability in these two seasons: five weather patterns in winter, and five in summer. Hence, the aCCFs which are currently available need to be seen as prototypes, and are strongly limited to their given geographic and seasonal coverage, i.e. being representative for the NAFC in summer and winter.

2.3 Enhanced aCCFs – Development of educated guess aCCFs

EUROPEAN PARTNERSHIP

Co-funded by the European Union

For the set of case studies for the year 2018, that are performed in WP2 and WP3 of the FlyATM4E project, an updated set of aCCFs was generated considering the current level of scientific understanding of aviation's climate effects which is described and defined in an educated guess [11].

As described above, an initial set of prototypic aCCFs is available, which has been derived from numerical simulations with Lagrangian air parcel trajectories focusing on the North Atlantic Flight corridor region in winter and summer. The recent publication of [8] presents this first consistent set of prototypic aCCFs formulas describing direct water vapour effects, NO_x induced effects and contrail cirrus together with the CO_2 effects (aCCF-V1.0). Additionally, [8] presents an implementation of aCCFs in the modular global chemistry-climate modelling system EMAC [36]. Within FlyATM4E, a new version of aCCFs was developed (aCCF-V1.1 [11]), which can be seen as one realisation within the range of plausible values (event horizon) considering the current level of scientific understanding of climate effects of aviation and their associated uncertainty. Such uncertainties can typically be described with probability distributions while defining the shape by the specific type (e.g. uniform, normal distributed, or logarithmical normal distributed) and the corresponding spread of the distribution resulting in an interval of values corresponding to the specific level of confidence (e.g. 90%, 95%, 99%, two-sided). For the construction of this educated guess in an initial step, climate effects of a full European airtraffic sample were evaluated by the prototype aCCFs, which are applied in the global chemistry model EMAC that is coupled to the airtraffic simulator AirTraf [31]. Consistently, the climate response model AirClim [21] was applied for the same European airtraffic sample, in order to provide an estimate of the associated climate effect on an annual mean basis. By comparing both estimates on an annual basis, a set of weighting factors were identified and applied to generate the educated guess. This consistent set of educated guess aCCFs (aCCF-V1.1, [11]) corresponds to the mean values of the respective uncertainty distributions when comparing the strength of effects calculated with the climate-response model AirClim and current literature, e.g. [1]. Departing from these mean values of aCCFs (educated guess), the range of possible, alternative values is explored in a risk assessment varying individual climate effects of aviation (hence their aCCFs) over the full range of possible values, as will be presented in more detail (see Section 2.5) after an overview on prevailing uncertainties in the current estimates of climate effects of aviation (see Section 2.4).

2.4 Characterisation of uncertainties in aCCFs

This section describes the uncertainties which are underlying the quantification of the aCCFs arising from different sources of uncertainties comprising atmospheric variability, limited predictability, and a low level of scientific understanding from climate science. The concept of characterising uncertainties responds to requirements from the application of aCCFs during trajectory optimisation (e.g. WP2) as the robustness of identified mitigation gains can be explored in a systematic risk analysis relying on a Monte-Carlo Method.

As described above, the spatial and temporal distribution of aCCFs specifies the climate effect of a local aviation emission via changes in CO_2, water vapour, ozone, and methane concentrations as well as contrail-cirrus effects. However, uncertainties associated with the calculation of these aCCFs prevail and need to be described by systematically exploring these specific sources of uncertainties and combining them with each other. In this section, we provide an overview of all individual sources of uncertainties together with a brief description of the origin of these uncertainties. In order to identify robust climate mitigation solutions and trajectories, adequate implementation of the most important individual sources of uncertainty in the systematic risk analysis is needed with an adapted complexity (see Section 2.5).

EUROPEAN PARTNERSHIP

Co-funded by the European Union

We distinguish (Table 1) between uncertainties related to (a) meteorological forecast, (b) calculation of climate impact, (c) development of aCCFs, and (d) emission calculation. Each group can be further broken down into individual sources. The (a) meteorological forecast is an important source of uncertainty, which is closely related to the forecast quality. Atmospheric variability in meteorological fields is causing a major challenge in reliably predicting atmospheric conditions and is highly impacting regions with strong or low climate effects, e.g. contrail forming regions. Thus, meteorological fields at the location in which the aircraft flies, hence emissions occur, are only known within a specific range of uncertainty. This variation of the meteorological data causes a variation in the forecasted and calculated aCCFs. Within FlyATM4E, a concept to characterize this weather forecast-related uncertainty is explored by the use of an operationally available ensemble prediction system (EPS) weather forecast. EPS is a forecast in which both the initial conditions and the physical parameters of a numerical weather model are slightly modified from one ensemble member to the other. Typically, about 50 ensemble members are provided, with each member representing a possible realization of a meteorological situation [5]. The specific concept of how this was investigated within the case studies and exercises in FlyATM4E is presented below (section 2.5) and in Deliverable D2.2 [34].

Additionally, in the calculation of climate effects within state-of-the-art chemistry-climate models, an important set of sources of uncertainty prevails. Specifically, representation of atmospheric processes and background conditions, uncertainties related to the calculation of the overall climate impact (e.g. caused by the representation of atmospheric processes) as well as uncertainties related to engine emission calculations cause uncertainties in these calculations.

Table 1: List of sources of uncertainties for individual aCCFs and for their associated calculations on climate effect.

Source of uncertainty	Origin of uncertainty
Meteorological Forecast	
Quality of meteorological forecast	Weather forecast data contains deviation from real world situations measured by quality of the forecast and its skill.
Calculation of climate effects and impact	
Representation of atmospheric processes	Chemistry scheme (e.g. O_3 production), cloud parametrization, horizontal and vertical resolution.
Change in GHG concentration/contrails	Background (e.g. temperature bias in EMAC).
Radiative forcing (RF)	Estimate of RF depends on assumption of linearity for radiative transfer calculations.
Temperature calculation	Temperature change calculation depends on assumptions on efficacy and temporal evolution of emissions/RF.
Physical climate metric	Climate metric has to be appropriate for the targeted climate objective but should still allow some variation with respect to assumptions on

EUROPEAN PARTNERSHIP

Co-funded by the European Union

	background emission scenario/model, emissions evolution (pulse/sustained/future scenario), climate indicator (e.g. averaged temperature response), and time horizon (e.g. ATR20).
Development of Algorithms to represent CCFs (=aCCFs)	
Development of algorithms in aCCFs	Due to the fitting of CCF data to meteorology at the location of emission, imperfections in the relationships are identified.
Emission calculation in emission model	
Emission index/conversion merged aCCFs	Assumptions in emission model.

The uncertainties shown in Table 1 and described in detail in [11] are associated with:

- **Representation of atmospheric processes**

  Model representation in chemistry schemes (e.g. chemical ozone production), background concentrations, cloud parametrization, horizontal and vertical resolution (numerical diffusion), as well as background conditions comprising also e.g. temperature bias, influence the quantitative estimate of concentration changes of radiatively active species (greenhouse gas concentrations).

- **Estimate of radiative forcing and temperature change**

  The calculation of the radiative forcing (RF) associated with changing radiatively active species depends on the radiation scheme performed by radiative transfer calculations. The global temperature change is linearly linked to the RF, assuming a constant climate sensitivity parameter (see e.g. [6]). However, this assumption is not valid for all forcing agents, in particular for forcing agents that are spatially not homogeneously distributed (as, for example, contrails). These forcing agents have different so-called efficacies (a more detailed description of efficacies can be found in Section 3.3). An adequate way of assessing and describing the resulting uncertainty is related to the analysis of the model dependent climate sensitivity, which can be retrieved from analysis using existing data from model comparison initiatives, e.g. IPCC AR5 or CMIP6. Overall analysis shows that climate sensitivity varies not only with the forcing agent but also highly varies with different climate models. From the recent IPCC report (2017), a range of estimates can be extracted.

- **Choice of physical climate metric**

  As there is not only one single physical climate metric that can be used, it has to be appropriately selected for the targeted climate objective. Additionally, the metric calculation depends on assumptions on background emission scenario, radiative transfer model and emissions evolution (pulse or sustained) or, alternatively, on a future emission scenario, which proxy data is used as climate indicators, such as averaged temperature response (ATR) at the surface or the selected time horizon (e.g. 20, 50, 100 years).

Moreover, due to the statistical based approach that was used to develop the aCCFs [2], additional uncertainties are introduced in the overall calculation. Correlations were identified by a systematic

analysis of correlations between estimated CCFs and the meteorological variables at the time of emissions. Hence, due to the fitting of CCF data to meteorology at the location of emission, imperfections in the relationships have been introduced, which lead to an overall uncertainty.

Finally, as the fourth group of uncertainties (see Table 1), assumptions on emission index and the associated conversion of merged aCCFs from trace gas emission related values (e.g. per kg NO_x emitted) to fuel related quantities (per fuel burn) introduces another uncertainty, which is directly related to the applied emission model and fuel flow estimates.

2.5 Concept towards robust aCCFs by integrating uncertainties

As described above, current scientific understanding of aviation's climate impact still recognizes uncertainties in the quantitative estimates in weather forecasts and climate impact prediction (see Section 2.4). Hence, FlyATM4E developed concepts on how to integrate individual uncertainties by means of the specifically identified approach to achieve robust aCCFs (R-aCCFs). Specifically, the overall concept relies on combining different types of uncertainty assessments in the overall modelling chain. First, using alternative models in order to evaluate and calibrate possible options within the range of uncertainties. Second, the statistical method of a Monte-Carlo variation was applied (Section 2.5.1) to describe and subsequently combine values with a quantified range of uncertainty. Third, dedicated sensitivity studies can be performed (Section 2.5.2) in order to perform an uncertainty assessment, as done e.g. by an ensemble prediction system for meteorological forecast uncertainties or distinct climate metrics. These specific options for expanding the aCCFs to R-aCCFs in the implementation by additional information have been explored [11], and concepts are presented in this section. The corresponding publication is in a final state and submission is scheduled for July 2022.

Different sources of uncertainty require individual concepts in order to integrate such additional information into the novel concept of R-aCCFs. Distinct options of implementation exist and how to integrate this comprehensive information on uncertainties and associated uncertainty ranges.

- First, educated guess estimates of aCCFs were developed (aCCF-V1.1), which represent possible representations within the event horizon of the generalized parameter domain which practically aligns these aCCF quantities to state-of-the-art research. As described above, this is done by evaluating, e.g. a reference case using alternative numerical models (here we use the climate-response model AirClim [21]), to provide a comparision on the climate effects of aviation as quantified by the overall approach. A detailed description, visualisation, and application of these educated guess aCCFs, which are mathematically equivalent to aCCFs, is given in [11].
- Second, a Monte-Carlo analysis can be performed once alternative trajectory solutions have been identified. By varying individual parameters over the parameter space, associated performance indicators and associated mitigation benefits are explored, resulting in an interval of possible values and, e.g., percentile as upper and lower limits.
- Third, aCCFs can be expanded by adding an additional dimension of information from dedicated sensitivity studies, e.g. by using individual members from an EPS forecast, by applying a different set of climate metrics, or results from further specific sensitivity studies. Representing uncertainties comprise different sources, e.g. weather forecasts, which is described in the following. State-of-the-art aCCFs are evaluated for different ensemble members within the EPS weather forecasts, and the distribution of aCCF values is analysed, providing, e.g. statistical percentiles and augmented with additional uncertainties arising from climate impact prediction. This leads to a time and location dependent uncertainty estimate in the aCCFs, which adds an

EUROPEAN PARTNERSHIP

Co-funded by the European Union

additional dimension to aCCFs while serving as a first input component resulting in a robustness-indicator (research goal of WP1).

2.5.1 Quantification of uncertainties by statistical methods

Statistical description of individual sources of uncertainties relies on the provision of the underlying mathematical distribution (e.g. normal, logarithmic normal, uniform), the corresponding mean or median values as well the lower and upper limit of the uncertainty interval. The uncertainty ranges and distributions used to characterise the individual sources of uncertainties are provided in Table 2. They are based on state-of-the-art research [1] [21] and have also been applied in [11]. In the following, brief explanations for a set of aggregated sources of uncertainty are provided:

- **Uncertainty range for radiative forcing**

  As shown in Figure 1 large uncertainties arise from the radiative forcing estimate of non-CO_2 emissions of global aviation. Table 2 provides the respective uncertainty ranges of the RF of different radiative active species. The main uncertainties arise from NO_x induced ozone and methane and from contrail RF. For example, the contrail RF reveals an uncertainty range of about 70%. In contrast the uncertainty of water vapour RF is quite small. Overall uncertainties in the RF estimates of aviation consider a large number of state-of-the-art RF estimates derived from different climate models. These models differ, for example, in their radiative transfer scheme, in their representation of chemical processes or in their parameterizations of cloud microphysics. Moreover, the model setups (e.g., vertical and horizontal resolution or background scenario) can be different. Thus, the uncertainty source related to the representation of atmospheric processes (see Table 1) is included in these radiative forcing uncertainty ranges. Note, moreover, that these RF values refer to *global* climate impact of aviation emissions. For individual emission locations, these uncertainties can vary.

- **Uncertainty range for climate sensitivity**

  The above-mentioned uncertainties of aviation induced radiative forcing are large, but if converting the RF estimate to global annual mean near-surface temperature response (as done for the aCCFs), the uncertainty even increases. The global temperature change is linearly linked to the RF via the climate sensitivity parameter λ (for more details see Section 3.3). However, this climate sensitivity parameter highly varies with the used climate model and with the specific forcing agent. The dependency on forcing agents can be solved by using forcing efficacies. Uncertainty ranges have been estimated: the range in the climate sensitivity (variation with model and with forcing agents) will be given according to state-of-the-art research in accordance with [21].

2.5.2 Quantification of uncertainties by sensitivity studies

As an alternative to the evaluation of uncertainties according to a statistical distribution of values which has been shown above, it is also possible to estimate uncertainties by dedicated sensitivity studies. This means that in order to explore variation of key variables, individual realizations (e.g. a numerical experiment with varying parameters) are applied in the overall assessment. Within FlyATM4E, this approach is applied to explore the uncertainty of the **meteorological forecast**, i.e. by exploring individual members from an ensemble forecast system (see Section 4.5). In a similar way, distinct **climate metrics** can be explored by sensitivity studies, applying various climate metrics (e.g.

EUROPEAN PARTNERSHIP

Co-funded by the European Union

average temperature response, global warming potential, global temperature potential) over various time horizons. It has to be noted here that in FlyATM4E, the overall concept of trajectory optimization relies on the application of a single metric during trajectory optimization, while in a second modelling step, alternative physical climate metrics are employed. They should investigate the sensitivity of the overall mitigation gain in relation to the physical climate metric used in the performance assessment of climate effects.

- **Meteorological forecast using an ensemble prediction system (EPS)**

  As mentioned earlier, to represent the variability (and uncertainty) of the meteorological forecast, an EPS forecast can be used, which provides for a given day an ensemble of possible realisations of the meteorological conditions. In FlyATM4E, ten ensemble members from the ensemble prediction system are applied for the trajectory optimisation (WP2). Each ensemble member represents a possible, consistent realisation of the meteorological conditions, in which aircraft trajectories can be optimized. Alternatively from such an ensemble, the ensemble mean and its statistical standard deviation can be calculated, resulting in, e.g., mean temperature or mean relative humidity.

- **Climate effect measured by a climate metric**

  The selection of the physical climate metric introduces another source of uncertainty, which can well be explored by dedicated sensitivity studies. Any climate metric (targeting on temperature change) is composed by an emission scenario, a time horizon and a climate indicator (see also Section 3.3). aCCFs in FlyATM4E are based on the climate indicator ATR20 and the emission scenario is either based on pulse emission or on a future emission scenario. Although the choice of a climate metric is largely controlled by the climate objective [21], possibilities to adapt the details of the climate metric with regard to the time horizon, emission evolution and climate indicator exist. In order to allow exploring different climate metrics, a Python Library has been developed within the project, which allows the selection of distinct climate metrics by namelist settings.

As mentioned in the last section, another source of uncertainty arises also from the development of aCCFs, which rely on statistical correlation methods. However, related uncertainty can only be roughly estimated. Moreover, the uncertainty arising from different engine/aircraft combinations will also be addressed by using different aircraft dependent emission indices (see Section 3.2).

2.5.3 Towards implementation of uncertainties

When implementing spatially and temporally resolved information on climate effects of aviation emissions, it is key to ensure that prevailing uncertainties enter the overall modelling chain. As described above, the development of R-aCCFs relies on the combination of the adequate methods for the individual sources of uncertainty. Hence, FlyATM4E combines comprehensive information resulting from statistical methods, but also sensitivity studies in an integrative approach to provide an expanded vision on the climate effects and their uncertainty in a MET service comprising uncertainty information.

In the comprehensive assessment performed for a set of case studies during the year 2018, a further expanded concept towards robust aCCFs, which takes a smaller set of the above-mentioned ambiguities into account has been implemented. The option, which is currently proposed to represent these uncertainties towards robustness, relies on a set of aCCFs that considers educated guess

EUROPEAN PARTNERSHIP

Co-funded by the European Union

estimates using best guess estimates of individual climate impacts (here the basis is the conservative estimates of RF). Additionally, the second set of aCCFs is provided in order to perform individual risk analysis originating from different sources of uncertainty (see Table 1). This is done by quantitatively estimating the interval and error, if a lower or higher climate impact of e.g. contrail or NO_x is assumed. The quantification of this error can e.g. be based on the RF confidence interval given in Figure 1. Using that, lower range and higher range estimates can be calculated which can be combined to an overall uncertainty interval, forming the basis for a risk analysis. Departing from the mean values of aCCFs (educated guess as introduced in Section 2.3) the range of possible, alternative values is explored in a risk assessment varying individual aviation effects (hence their aCCFs) over the full range of possible values. Such variation of individual effects within their uncertainty ranges assesses the full range of possible combined total climate effects of aviation. At the same time, this variation determines to what extent potential benefits on alternative trajectories are robust in their mitigation of total climate effects. Such a systematic variation of individual coefficients over the full parameter space is performed by means of a Monte-Carlo variation analysis.

Table 2: Uncertainty ranges for the individual species given for different sources of uncertainties and different forcing species. For the radiative forcing (RF) and the climate sensitivity parameter (λ), the median, the upper and lower limit of the 95% likelihood is given together with the underlying distributions. Estimates are based on [1] [21].

	Statistical value	**CO_2**	**water vapour**	**ozone**	**PMO**	**methane**	**Contrail-cirrus**
RF	Distribution	Normal	log normal	log normal	log normal	log normal	Normal
	Minimum	31	0.8	23	-17	-34	33
	Median	34.3	2.0	36.0	-9.0	-17.9	111.4
	Maximum	38	3.2	56	-6.3	-13	189
λ	Distribution	Normal	log normal	log normal	log normal	log normal	log normal
	Minimum	0.69	0.58	0.70	0.77	0.77	0.39
	Median	0.73	0.83	1.00	0.86	0.86	0.43
	Maximum	0.77	1.08	1.3	0.95	0.95	0.47

We have applied this concept for the first time within the FlyATM4E aircraft trajectory optimization study (see D2.2 [34] and D3.2 [33], [11]). The corresponding experiment design relies on one reference optimization using the educated guess aCCFs and sensitivity experiments that quantify the “forgotten impact” by using the low- or high-aCCFs estimates. A robust trajectory is characterized by not losing overall mitigation gains even if lower or upper estimates of aCCFs are applied.

EUROPEAN PARTNERSHIP

Co-funded by the European Union

3 Generating merged aCCFs

In this section, it is described how the individual spatial and temporal resolved aCCFs of water vapour, NO_x-induced ozone and methane and contrail cirrus are combined to a merged non-CO_2 aCCF. By considering the actual synoptical condition and technical specification of the engine/aircraft type, and of the physical climate metric such merged non-CO_2 aCCFs can be generated. Technically this is done using a Python Library (see Section 3.4).

This section mainly includes results and descriptions from the scientific paper "A python library for calculating individual and merged non-CO_2 algorithmic climate change functions" [10], which is in preparation and will be submitted in July 2022.

3.1 Concept of generating merged aCCFs

Based on aCCFs that represent the individual effects of water vapour, NOx induced ozone and methane changes and contrail cirrus, a single aCCF function which combines these individual non-CO_2 impacts is generated (i.e. merged aCCF). This merged aCCFs can be used as advanced MET information for flight planning, as a climate optimal trajectory requires the quantification of the total non-CO_2 climate impact as four-dimensional data set (latitude, longitude, altitude and time). Therefore, all individual aCCFs must be converted to the same unit [K/kg(fuel)]. To do so, emission indices and the choice of consistent climate metrics are needed. In the following, we describe the concept of merging and the underlying assumptions in detail.

To this end, emission indices for NO_x (EI_{NOx} in g/kg(fuel)) and for contrail cirrus, the specific range (F_{km}) in [km/kg(fuel)] is required. Note that the water vapour aCCF formula is fuel related and thus doesn't need to be multiplied with the emission index of water vapour. Typically averaged fleet mean values of EI_{NOx} and F_{km} for transatlantic flights are available from the literature: fleet mean values for F_{km} and EI_{NOx} are 0.16 km/kg(fuel) ([15] and personal communication F. Linke, TU Hamburg, 2020) and 13 g (NO_2)/kg(fuel) [14], respectively. Another possibility is to take specific emitted amounts of NO_x emissions and specific range values from an engine performance model (see Section 2.3). With these emission indices it is possible to generate merged non-CO_2 aCCFs ($aCCF_{merged}$) in [K/kg(fuel)]:

$$aCCF_{merged} = aCCF_{NOx} * EI_{NOx} + aCCF_{contrail} * F_{km} + aCCF_{H2O}$$

Overall, merged aCCFs can vary with the chosen emission index and climate metric. Thus, we intend to provide merged aCCFs, which consider the actual weather situation, the aircraft specific data (e.g. aircraft/engine type, cruise altitude) and the physical climate metric. For an efficient and flexible provision of merged aCCFs, we have developed the Python Library (see Section 3.4)

3.2 Choice of emission index

The assumption of constant typical fleet mean values for F_{km} and EI_{NOx} for transatlantic flights represents a simplification, as the emission index depends on the flight level, and the aircraft/engine type. To consider the cruise altitude dependency and engine/aircraft dependency, we provide aggregated fleet-level values for EI_{NOx} and the specific range for a variety of aircraft types. These specific EI_{NOx} and F_{km} values are computed based on the EUROCONTROL-modified Boeing Fuel Flow method 2 [16][17] using engine performance characteristics given by EUROCONTROL's Base of Aircraft

EUROPEAN PARTNERSHIP

Co-funded by the European Union

Data (BADA, [18]). As the values from aircraft types that can be assigned to a certain class (Regional: small aircraft with short range (up to 100 seats), Single-Aisle: short to medium-range narrow-body aircraft, Widebody: medium to long-range aircraft (250-600 seats)) are similar, we group those aircraft types and provide average fleet values in Table 3 and Table 4.

Table 3 clearly shows that average EI_{NOx} values increase with increasing aircraft class/size and decrease with increasing altitude. NO_x emissions are produced during combustion due to high combustion temperatures, which are connected to high thrust settings and engine load conditions. There is a correlation between aircraft mass and engine thrust requirement, so that also combustion temperatures might rise with increasing aircraft size. Below cruise altitude, the aircraft is e.g. during climb operated with climb thrust and during descent with near idle conditions leading to, on average, higher engine loads at lower altitudes than during cruise. The specific range in Table 4 increases with altitude, as the aircraft is operated in near-fuel-optimal conditions during cruise. On the other hand, a larger aircraft tends to have a lower specific range than a smaller aircraft, as an aircraft becomes less fuel efficient on longer ranges, on which it has to carry additional fuel solely for the purpose of transporting a higher fuel mass over a long distance.

The calculation of merged aCCFs that consider these engine/aircraft dependent emission indices is technically solved with the help of the Python Library (see Section 3.4).

Table 3: Average specific NOx emission indices (in g(NO2)) for three aircraft classes (regional, single-aisle, widebody) derived from the emission inventory of the DLR project "Transport and Climate" (TraK). EINOx are shown for various typical flight altitudes (20000 ft - 40000 ft). Besides the flight altitude in ft, the corresponding pressure level is given in hPa. Table taken from submitted publication [10].

flight altitude [ft]	pressure level[hPa]	Regional [g(NO_2)]	Single-Aisle [g(NO_2)]	Wide-body [g(NO_2)]
20000	466	11.628	17.279	24.750
25000	376	10.223	14.877	22.182
30000	301	9.377	13.603	19.158
35000	238	7.968	11.249	15.008
40000	188	6.567	8.564	12.730

Table 4: Average flown distance per burnt fuel(km/kg(fuel)) for three aircraft classes (regional, single-sisle, widebody) derived from the TraK emission inventory. EINOx is shown for various typical flight altitudes (20000 ft - 40000 ft). Besides the flight altitude in ft, the corresponding pressure level is given in hPa. Table taken from submitted publication [10].

flight altitude [ft]	pressure level [hPa]	Regional [km/kg(fuel)]	Single-Aisle [km/kg(fuel)]	Wide-body [km/kg(fuel)]
20000	466	0.393	0.252	0.096
25000	376	0.442	0.282	0.107
30000	301	0.470	0.287	0.117
35000	238	0.488	0.324	0.120
40000	188	0.682	0.401	0.157

EUROPEAN PARTNERSHIP

Co-funded by the European Union

3.3 Choice of climate metric and efficacy

Physical climate metrics can be understood as a method that allows a direct and fair comparison across different forcing argents as well as across different sectors and sources [19]. A climate metric is a combination of climate indicators (e.g. average temperature response (ATR) or greenhouse warming potential (GWP)), time horizon (e.g. 20, 50 and 100 years) and emission scenario (including emission course and background emission) [19]. As emission scenarios, a pulse, sustained or a future scenario might be considered [20]. An adequate metric for assessing the mitigation of climate impact is for example the average temperature response over 20 years given for an increasing future emission scenario (F-ATR20) or a pulse emission (P-ATR20).

For generating merged aCCFs, FlyATM4E uses a consistent set of individual prototype aCCFs [8]. These aCCFs are all based on the climate metric of ATR20. The emission scenario assumed in the individual aCCFs is consistently pulse emission. However, there are different options, assumptions and decisions to adapt the details of the climate metric with regard to time horizon, emission evolution, and climate indicator. Thus, we provide factors that allow to switch, e.g. from the P-ATR20 metric to other physical climate metrics., as e.g. F-ATR20, F-ATR50, F-ATR100. A set of conversion factors was calculated for reasonable climate metrics with the help of the climate response model AirClim [21]. This set of conversion factors is given in Table 5.

Table 5: Climate metric conversion factors from P-ATR20 (pulse emission over time horizon of 20 years) to F-ATR20 (increasing future emission scenario over time horizon of 20 years), F-ATR50 (increasing future emission scenario over time horizon of 50 years), and F-ATR100 (increasing future emission scenario over time horizon of 100 years), for water vapour, ozone, methane, PMO, contrail cirrus and CO_2 aCCFs. Table taken from submitted publication [10].

	F-ATR20	F-ATR50	F-ATR100
water vapour aCCF	14.47	34.13	58.34
ozone aCCF	14.47	34.13	58.34
methane aCCF	9.83	41.48	97.37
PMO aCCF	9.83	41.48	97.37
contrail aCCF	13.42	29.46	47.31
CO_2 aCCF	9.28	43.92	124.93

As mentioned above, the global mean surface temperature changes using a model dependent constant, the so-called climate sensitivity parameter [22]. For radiative active gases with a distinctly inhomogeneous structure as e.g. ozone and contrails, the relation with constant climate sensitivity parameter fails (e.g. [22]). A way to account for this, is to introduce forcing dependent efficacies (leading to an effective RF) [1][22]. The prototype aCCFs formulations of [8] are given without taking the efficacy of the different non-CO_2 agents into account. However, integrating the efficacies of water vapour, ozone and methane to the merged aCCFs makes the prediction of aviation climate impact more reliable. State-of-the-art efficacies are summarized in Table 6. The efficacy of the NO_x induced short term ozone is 1.37 and the efficacy of the NO_x induced methane is 1.18. This means that radiative

EUROPEAN PARTNERSHIP

Co-funded by the European Union

forcing from ozone and methane has a higher impact on the temperature response than radiative forcing from CO_2. For contrails, the efficacy is estimated to amount to 0.42, meaning that contrail RF has a lower impact on the global temperature response than CO_2. The value of the contrail efficacy estimate of [1] is the combination (mean) of three different contrail efficacy estimates from earlier studies, including estimates of 0.59 [24], 0.31 [25] and 0.35 [26].

Table 6: Overview of state-of-the-art efficacies of NO_x induced ozone, methane, primary mode ozone (PMO), as well as water vapour and contrails. Respective references are given in the right side of the table.

	efficacy	Reference
ozone	1.37	Ponater et al. (2006)
methane	1.18	Ponater et al. (2006)
PMO	1.18	Lee et al. (2021)
H_2O	1	Lee et al. (2021)
contrail-cirrus	0.59	Ponater et al. (2005)
	0.31	Rap et al. (2010)
	0.35	Bickel et al. (2020)
	0.42	Lee et al. (2021)

* Lee et al. 2021 value is the mean over the values given by Bickel et al. (2020); Ponater et al. (2005); Rap et al. (2010)

3.4 Technical implementation of individual and merged aCCFs using a Python Library

FlyATM4E developed the open-source Python Library CLIMaCCF (available on Zenodo with the software DOI: 10.5281/zenodo.6977272), a flexible and intuitive tool, that efficiently calculates both the individual aCCFs (i.e. water vapour, NO_x induced ozone and methane and contrail-cirrus aCCF) and the merged non-CO_2 aCCFs. As described above, these merged aCCFs can only be constructed with the technical specification of the emission indices of the selected engine/aircraft type. Overall, the scope of CLIMaCCF is to provide merged aCCFs as spatially and temporally resolved information considering the actual synoptical situation, the engine/aircraft type, the physical climate metric and the prototype algorithms in individual aCCFs.

In the following, some details on the technical implementation of the Python Library are presented. The Python Library consists of three main blocks: input, processing and output (see the schematic workflow in Figure 2). In the input block, the Python Library receives weather data (e.g. weather forecast, reanalysis data, etc.) containing the required meteorological input. In the processing block, the individual aCCFs are calculated and merged aCCFs are generated by taking specific assumptions on engine/aircraft type and climate metric. In the output block, the individual and merged aCCFs are stored.

EUROPEAN PARTNERSHIP

Co-funded by the European Union

Figure 2: Schematic workflow of calculating merged aCCFs using the Python Library CLIMaCCF. The left row describes the Input block, the top raw the processing block and the bottom raw the output block [10] .

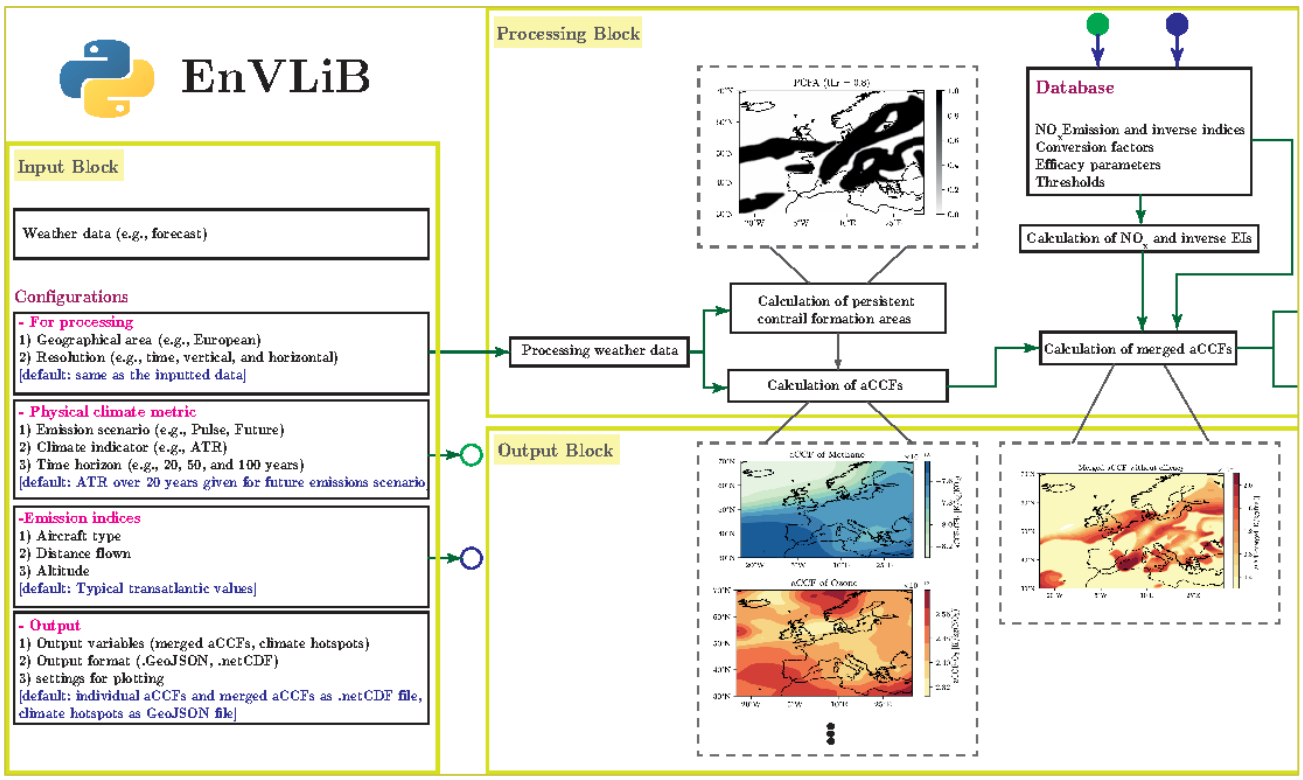

Input block

Within the input block, the meteorological input data for the aCCFs calculation are specified by the user. All meteorological input data needed to calculate the individual aCCFs are summarized in Table 7. The current implementation of the library is compatible and tested with the standard of the European Centre for Medium-Range Weather Forecasts (ECMWF) data.

Table 7: Meteorological input parameter to calculate aCCFs within CLIMaCCF

Meteorological variables
Potential vorticity unit [10^{-6}K · m^2/kg · s]
Relative humidity [%]
Outgoing longwave radiation (OLR) [W/m^2]
Incoming solar radiation at top of the atmosphere [W/m^2]
Temperature [K]
Geopotential [m^2/s^2]

The user has the possibility to choose between different configuration settings as different assumptions for the physical climate metric: emission scenario, and time horizons (default is P-ATR20). Moreover, the user can decide if the calculation of merged aCCFs is performed with or without considering efficacies. As the selection of aircraft/engine type is an important factor in determining reliable merged aCCFs, the database of the library has implemented an initial set of specific emission

EUROPEAN PARTNERSHIP
Co-funded by the European Union

indices for selected aggregated aircraft/engine combinations. By selecting the aircraft type, the altitude dependent NO_x emission indices and flown distances kg burnt fuel are calculated for the user.

Processing block

This block performs main calculations using the given meteorological input data and the above-described user configurations. The individual aCCFs are calculated by the formulas provided in Appendix A. Merged aCCFs are combined based on metric conversion factors, efficacy, and emission indices.

Output block

The processed climate change functions are saved within this block. Currently, the library supports two standard data formats. One is netCDF for saving aCCFs, and the other one is the GeoJson format.

EUROPEAN PARTNERSHIP

Co-funded by the European Union

4 Systematic analysis of individual aCCF patterns

This section delivers a comprehensive analysis of characteristics and variability of individual and merged aCCFs. First, we illustrate how the spatially and temporally resolved climate impact of individual aviation emissions looks like by showing prototypic aCCFs in distinct weather situations over Europe of individual non-CO_2 effects (i.e. water vapour, NO_x, contrail-cirrus) using standard meteorological input data of ERA5 reanalysis data of typical summer and winter days in the year 2018. The individual aCCFs are calculated by using the mathematical prototypic formulas. These prototypic formulas currently contain the state-of-knowledge using base-simulations for the North Atlantic Flight Corridor. However, we recognize that this is a topic of ongoing research on state-of-the-art understanding on aviation's climate impacts. Hence, in the near future, it is expected to have a larger set of base-simulations available from ongoing research initiatives. These will enable to expand e.g. the geographic scope or season. Hence, prototypic aCCFs have been subject and will be subject to revisions and updates, requiring to publish on a regular basis these updated versions of aCCFs. Additionally, the aCCF formulation depends as well on a set of decisions and assumptions relating to policy and societal aspects, e.g. time horizon of the applied climate metric. Thus, this deliverable will explain current understanding and document implementation applied within the FlyATM4E project.

4.1 Description of calculated aCCFs

As mentioned above, the strength of the aCCFs is their sole reliance on relevant local meteorological parameters for their calculation. In the following theERA5 reanalysis data set [27], which was developed by the European Centre for Medium-Range Weather Forecasts (ECWMF) is used as meteorological input. They represent an atmospheric model system that assimilates surface and upper-air conventional and satellite data.

For the trajectory optimization in WP2, a set of summer and winter days was specified (for details see Deliverable D2.3 [34]). These days include five days in June 2018 (i.e. 13th, 15th, 18th, 23th and 27th June) and five days in December 2018 (i.e. 5th, 10th, 15th, 20th, 25th December). With this selection, different representative synoptic winter and summer situations are included. In order to describe these different weather conditions, the geopotential height and the wind fields are shown in Appendix B (Figure B1-B4).

The aCCFs presented in the following are based on a consistent set of prototype aCCF formulas (see Appendix A) and include educated guess factors, that were developed in the FlyATM4E project in order to represent aviation's climate impact in line with state-of-the-art research (see Section 2.4). Additionally, the aCCFs express the climate impact in terms of F-ATR20 (average temperature response over a time horizon of 20 years using the increasing future emission scenario BAU) and include efficacies. For merging, aCCFs need to be converted to the same unit of K/kg(fuel) This is done by assuming typical fleet mean values of EI_{NOx} and of F_{km} for transatlantic flights (see Section 3.1).

4.2 Characteristic aCCF patterns of specific winter and summer days

In this section, the prototypic aCCFs in distinct weather situations over Europe are shown, illustrating the spatial and temporal resolved climate impact of individual aviation emissions. Figure 3 provides

EUROPEAN PARTNERSHIP

Co-funded by the European Union

the characteristic summer patterns of water vapour, total NO_x (including ozone, methane and PMO impact) and daytime contrail-cirrus together with the merged non-CO_2 aCCFs. Note that all aCCFs are converted to the same unit of K/kg(fuel) by taking assumptions for the NO_x emission indices (for the total NO_x aCCF) and flown distance per burnt kg fuel (for the contrail aCCF). These aCCF patterns are shown at 250 hPa for daytime conditions (12 UTC) and give an impression of their typical geographical distribution over the European air space on several specific summer days (i.e. 13th, 15th, 18th, 23th and 27th June 2018) with distinct synoptical conditions. For these specific days, a weather pattern classification according to [28] (more details see Appendix B1.2) was applied and the respective classification is given on the right sight of each plot. The water vapour aCCF (Figure 3a) shows positive (warming) values and highly varies for the different synoptic situations The total NO_x aCCFs (Figure 3b) combines the positive (warming) ozone aCCFs and the negative (reduced warming, i.e. net-cooling) methane aCCFs. This can be explained by the fact that NO_x emission from aviation leads to ozone formation, and the methane aCCF is negative as NO_x emissions are destroying methane. Overall the total NO_x aCCF is positive and a zonal gradient can be observed with generally higher positive values in lower latitudes (Figure 3b). This can be explained by the higher ozone formation in lower latitudes. Moreover, the NO_x aCCFs show a high variation for the specific days, thus, they are highly influenced by the different weather situations. Daytime contrail cirrus aCCFs (Figure 3c) predict positive and negative values. This is explained by the shortwave and longwave radiative impact of contrails during day. During night contrails have only longwave radiative impact, thus the night time contrails aCCFs are positive only (see Figure B5 of Appendix B). As contrail formation and contrail climate impact are very sensitive to the atmospheric conditions, contrail aCCF shows a large geographical and day to day variability.

As described in Section 3, a merged aCCF can only be constructed with information on the aircraft-engine dependent values of NO_x emission and flown distance. In Figure 3 (d), the merged non-CO_2 aCCFs are provided together with the individual aCCFs (all given in K/kg(fuel)). Comparing the individual aCCFs to the merged aCCFs, it is clear that contrail aCCFs dominate the merged aCCF in structure and magnitude; NO_x induced aCCFs play also a role, whereas water vapour aCCFs are negligible. Thus, overall, we expect the highest mitigation potential in avoiding contrail-cirrus. Based on the merged aCCF pattern a climate optimized flight trajectory could probably calculate a compromise between avoiding long distances through enhanced climate warming areas and at the same time avoiding long detours as these would induce a penalty with respect to CO_2 aCCF.

EUROPEAN PARTNERSHIP

Co-funded by the European Union

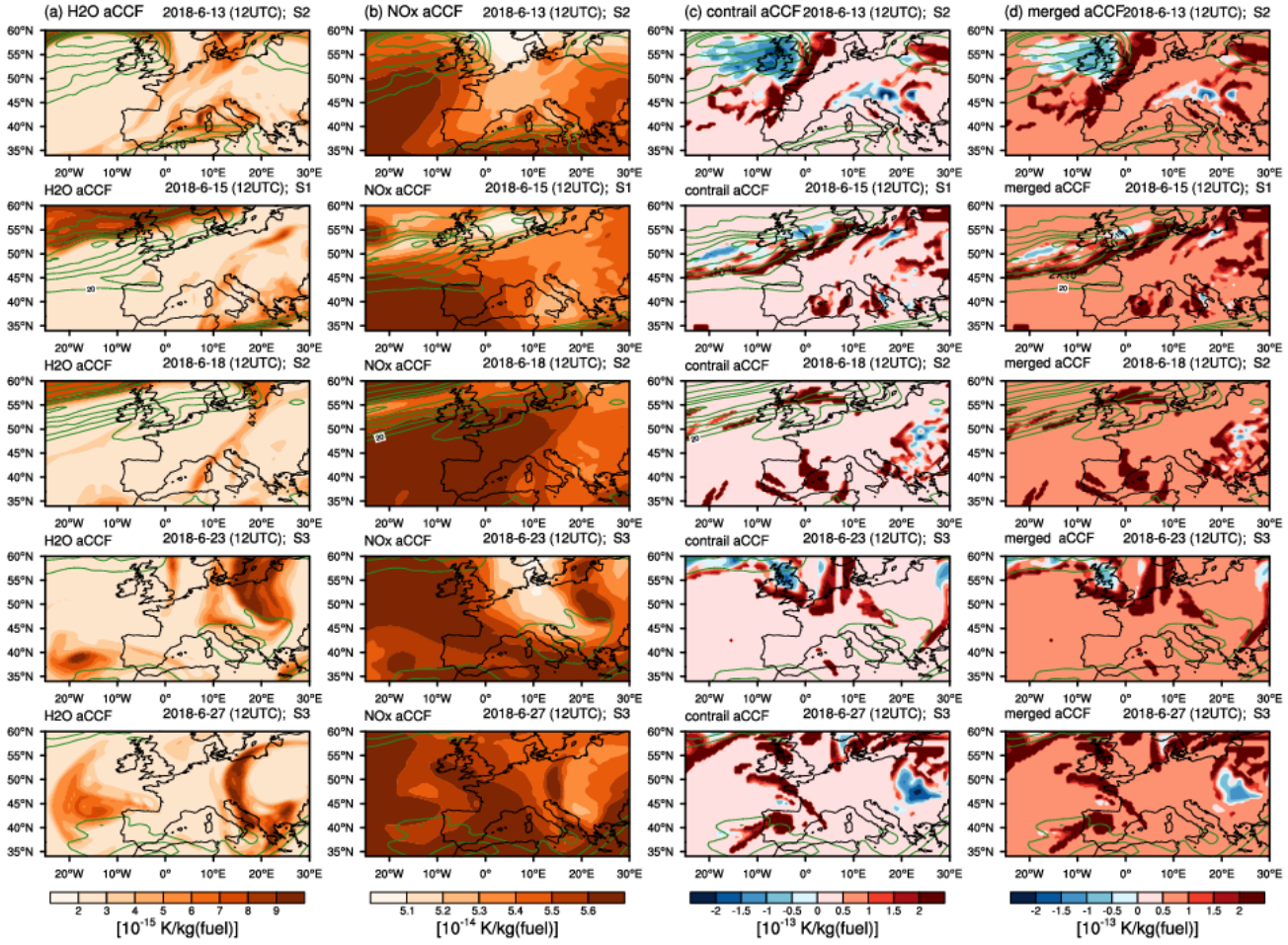

Figure 3: Characteristic patterns of (a) water vapour aCCF [K/kg($_{fuel}$)], (b) NO_x aCCF (including O_3, CH_4 and PMO) [K/kg(fuel)], (c) contrail (daytime) aCCF [K/kg(fuel)], and (d) merged non-CO_2 aCCF [K/kg(fuel)] at pressure level 250 hPa over the European region for five selected days in June 2018 at 12UTC. Individual aCCFs were calculated from ERA5 reanalysis data. Overlaid green lines indicate wind speeds above 30 ms^{-2}. The weather situation of the specific days was classified according to [28] and is given beside the date on the upper right.

4.3 Variation of aCCFs with season

In this section, we give detailed information on how the aCCF patterns vary with different seasons. Analogue to Figure 3, Figure 4 provides characteristic winter patterns of water vapour, total NO_x, contrails and merged aCCFs for daytime conditions. Again, the selected winter days (i.e. 5th, 10th, 14th, 20th, 25thDecember 2018) represent different typical winter synoptic conditions. Additionally, in Figure B6, the respective patterns for nighttime conditions are given.

Comparing the winter and summer water vapour aCCF pattern shows somewhat larger values for winter conditions. For the NO_x aCCFs, highest values can be found during the summer season. This is explained, as in summer NO_x emissions lead to higher photochemical ozone production. Investigating the seasonal variation of contrail aCCFs reveals generally less conditions for persistent contrail formation in summer and, therefore, less areas with cooling, i.e. contrails are supposed to warm more during summer.

EUROPEAN PARTNERSHIP
Co-funded by the European Union

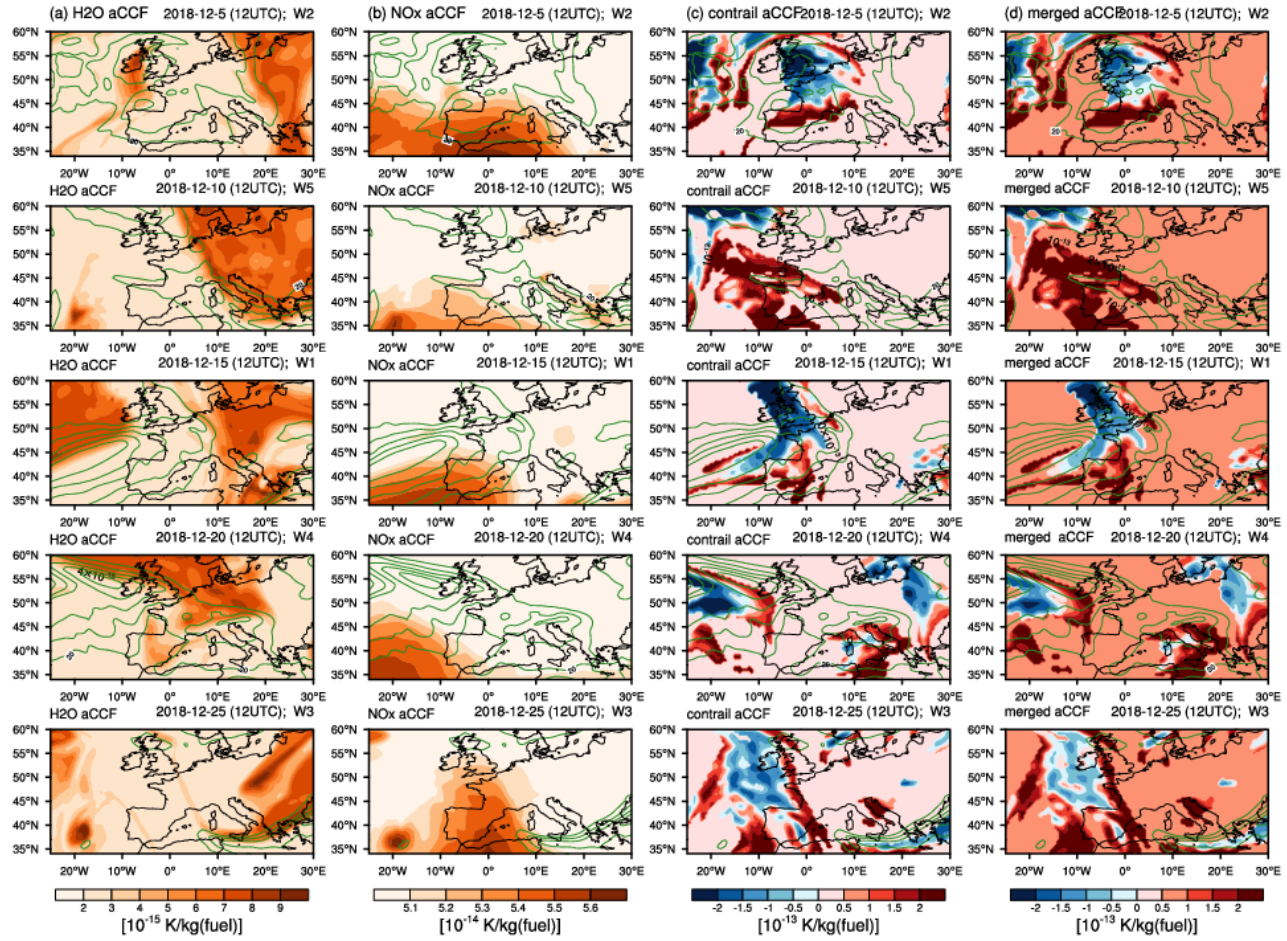

Figure 4: Characteristic patterns of (a) water vapour aCCF [K/kg($_{fuel}$)], (b) NO_x aCCF (including O_3, CH_4 and PMO) [K/kg(fuel)], (c) contrail (daytime) aCCF [K/kg(fuel)], and (d) merged non-CO_2 aCCF [K/kg(fuel)] at pressure level 250 hPa over European region for 5 selected days in December 2018, at 12UTC. Individual aCCFs were calculated from ERA5 reanalysis data. Overlaid green lines indicate wind speeds speeds above 30 ms^{-2}. The weather situation of the specific days was classified according to [28] and is given beside the date on the upper right.

4.4 Variation of aCCFs with cruise altitude

Several previous studies (e.g. [21], [30]) investigated the climate mitigation potential with cruise altitude, showing that the climate impact largely varies with flight altitude indicating that flying lower can reduce the non-CO_2 effects by about 30% [30].

To demonstrate the vertical structure of individual and merged aCCFs in the typical flight altitudes between 200 and 400 hPa, Figure 5 displays the vertical cross section along the longitude 0°E (located over Europe) in the northern hemisphere (0-60°N) for the five selected days in June 2018. The respective vertical structure of these five specific winter days is given in Appendix B 1.4 (Figure B7).

Water vapour aCCFs show high variation with cruise altitude. Generally, higher values can be found in higher altitudes. Regions with high amount in water vapour aCCFs mainly lie in the stratosphere, as water vapour that is directly emitted to the stratosphere has a high climate impact. The NO_x aCCFs show an increase in their climate impact (higher aCCFs) in the range 250 – 300 hPa. Moreover, an

EUROPEAN PARTNERSHIP
Co-funded by the European Union

increase of NO_x aCCFs from high to low latitudes can be found. The contrail aCCFs have a very variable vertical structure with negative and positive climate impact, that extends from 200 to 400 hPa. Overall, a strong contrail climate impact can be found in regions above 200 hPa. However, at higher latitudes, the extension of contrail aCCFs to lower altitudes is given, as contrail formation is linked to low temperatures. The vertical profile of the merged aCCF is highly dominated by gradients of the contrail aCCF.

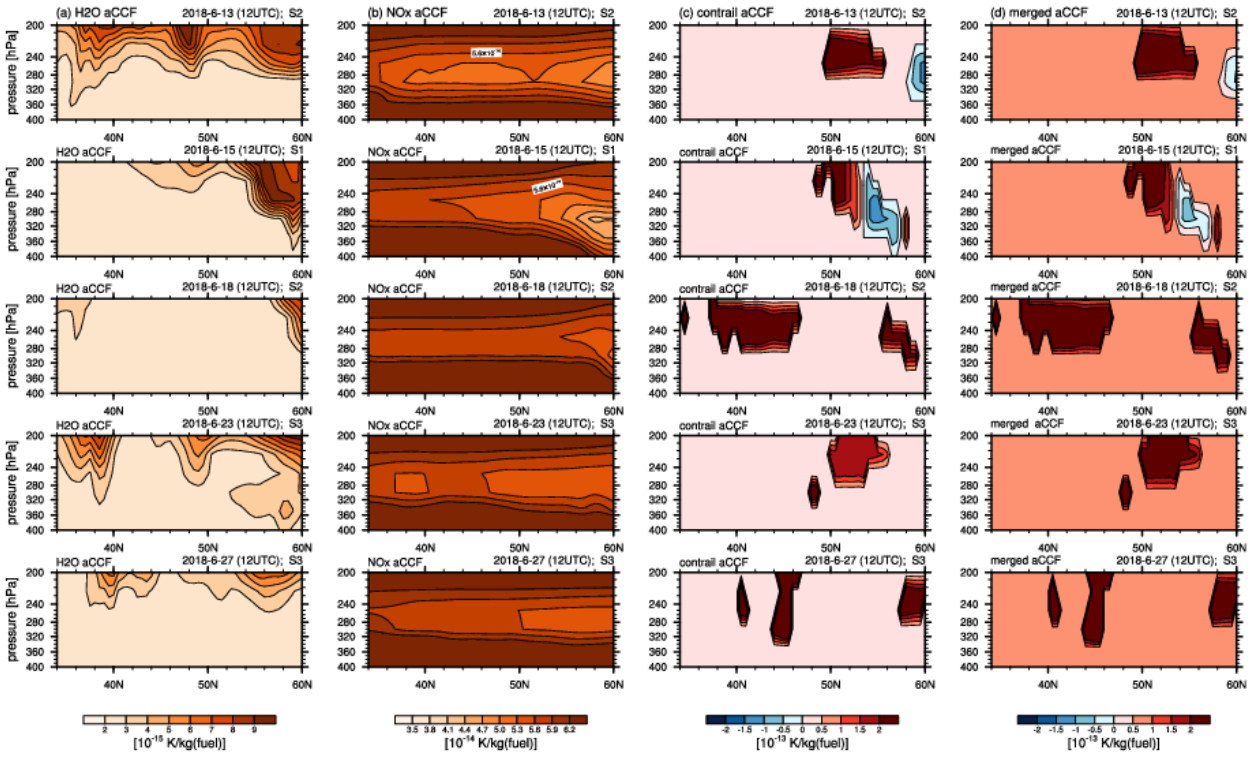

Figure 5: Vertical cross section patterns of (a) water vapour aCCF [K/kg($_{fuel}$)], (b) NO_x aCCF [K/kg(fuel)], (c) contrail aCCF [K/kg(fuel)], and (d) merged non-CO_2 aCCF [K/kg(fuel)] at longitude 0° for five selected days in June 2018 at 12UTC. Individual aCCFs were calculated from ERA5 reanalysis data.

4.5 aCCFs calculated from EPS weather forecast

As aCCFs rely on numerical weather prediction data that deviate from the real-world situation, aCCFs and thus studies on aircraft trajectory optimization will include uncertainties arising from MET information including forecast quality and skill. One possibility for exploring the quality and hence, uncertainty, of the weather forecast is to use an ensemble prediction system (EPS) weather forecast.

In FlyATM4E, the uncertainties from the meteorological forecast data are integrated into the aCCFs by using such an ensemble forecast. As these aCCFs include robustness aspects, they can be defined as robust aCCFs (R-aCCFs). Here we use the probabilistic EPS weather forecast from ECWMF to explore individual ensemble members and assess the performance of aircraft trajectories under different meteorological situations in order to explore the variability of the forecasted weather situations.

In Figure 6, the ensemble mean value (average over ensemble members) and the related disagreement between ensemble members (standard deviation of these ensemble members) is shown for the NO_x induced aCCFs (including the NO_x induced ozone aCCF and the NO_x induced methane aCCF) and for the

Co-funded by the European Union

contrail aCCF exemplary for the 13th of June 2018, 12UTC. The standard deviation of NO_x aCCFs along the ensemble members is quite low (compared to contrail aCCFs); only in certain regions, there are slightly higher variations between the ensemble members. Thus, robust mitigation of the NO_x climate impact should be possible. For contrails, however, the standard deviation of contrail effects is comparably high for any region with contrail effects forecasted because contrail formation is based on highly variable fields comprising temperature and relative humidity.

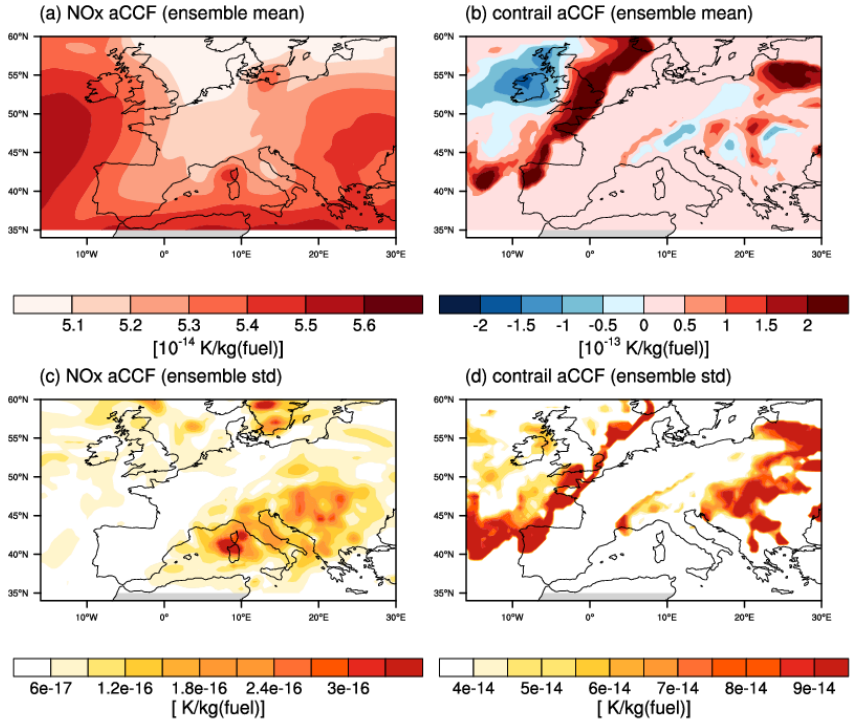

Figure 6: Characteristic patterns of the ensemble mean (a) NO_x aCCF [K/kg(fuel)] and (b) contrail aCCF [K/kg(fuel)]. The corresponding standard deviations are given for (c) NO_x aCCF and (d) contrail aCCF. All figures are displayed at pressure level 250 hPa over the European region on 13th June 2018, 12UTC. aCCFs were calculated from 50 ensemble members of an EPS weather forecast.

Based on these robust aCCFs, those weather situations and aircraft trajectories can be identified, which lead to a robust climate impact reduction (for more details see D2.2 [34]).

4.6 Guidance on and analysis of situations with high mitigation potential

In this section, we analyse aviation's climate effects (in terms of aCCFs) for areas and seasons, which result in a large mitigation potential (i.e. eco-efficient solutions) and win-win solutions (detailed definition of eco-efficient and win-win see Deliverable D3.2 [33]).

Synoptic situations with large contributions from non-CO_2 effects offer a larger mitigation potential for climate-optimized trajectory planning. By analyzing the spatial and temporal distribution of merged non-CO_2 aCCFs, while comparing to the CO_2 effects, situations and regions with a larger mitigation potential can be identified. Such situations and regions are characterized by comparatively large merged non-CO_2 aCCFs. In contrast to this, situations with lower values of merged non-CO_2 aCCFs

EUROPEAN PARTNERSHIP
Co-funded by the European Union

indicate, that during such situtations or in those regions the total climate effects are comparably lower, as associated non-CO_2 effects are lower as well. Similarly, analyzing the climate effects of aircraft operations resulting from a fixed set of city pairs during the course of the year, identifies seasons with larger non-CO2 effects and hence higher mitigation potentials (as shown below).

In WP3 of FlyATM4E, the air traffic simulator AirTraf [31] coupled to the global chemistry climate model EMAC [36] was used to explore climate-optimized trajectories and estimate their mitigation potential during the course of a year (here specifically for the year 2018). AirTraf applies a defined routing strategy during a one-year simulation of the global atmosphere and associated aircraft movements for a specific set of city-pairs (for details see Deliverable D3.2 [33]). Analysis of the seasonal dependence of the average temperature change over 20 years of a traffic sample containing 100 flights (calculated with the help of the aCCFs, see Section 4.3) shows a clear seasonal dependence of aviation's total non-CO_2 effects. For example, high effects can be found in June but also in late summer resulting from the NO_x-induced climate effects. Comparing such seasonal dependence with analysis from aircraft trajectory optimizations from WP3 identifies also seasonal dependence of mitigation gains which follows the seasonal dependence of the total climate effects, e.g. F-ATR20. The temporal evolution of the average climate effect of aviation (ATR20) from the cost optimal (simple operating costs SOC) and eco-efficent trajectory solutions (i.e. trajectories and respective meteorological situations which allow a substantial reduction in climate impact of a flight, while leaving its cost nearly unchanged) are investigated, identifying regions and seasons with high non-CO_2 effects and associated high mitigation gains (see Deliverable D3.2 [33], therein Figure 6). Based on this figure, it is clear that the mitigation gain of the eco-efficient trajectory optimization strategy varies throughout the year, with winter months having higher mitigation potential than summer months. Relative mitigation gains show a strong seasonal dependence, with high relative reductions in winter for the day-time flights, and a high relative reduction in June and late summer for night-time flights.

Moreover, beyond such large mitigation potentials due to high non-CO_2 effects, it is also of high interest to identify to what extent a mitigation potential in a win-win situation exists by eliminating a constrain. Within the FlyATM4E project, the case studies performed allow for assessing the relevance of the constrain due to the usage of two distinct trajectory optimizers, ROOST (Robust Optimisation of Structured Airspace) and TOM (Trajectory Optimisation Module). ROOST is a model which optimizes trajectories on a structured-airspace (using the current network of Air Traffic Services routes) [35], and TOM is a trajectory optimizer that uses free-routing airspace (future concept of operations) [37]. Note that a detailed description of the trajectory optimizers ROOST and TOM will be given in D2.3 [34]. These expanded flight trajectory optimization tools identify and evaluate such optimized trajectories for specific weather situations. For a given day, the ensemble forecast data is used and while ROOST relies on the ensemble mean and its standard deviation for the stochastical optimisation, TOM is performing one optimization after the other. In ROOST, a unique "robust" flight path is identified with the help of the ensemble mean which is then evaluated in each of the ten ensemble members. By comparing cost optimal trajectories computed on a structured-airspace (using the current network of ATS routes) with climate optimal trajectories computed on a Free-Routing airspace (future concept of operations), win-win solutions can be identified in which both overall cost and overall climate impact can be reduced. Promising candidates for such win-win situations are expected to be also present in meteorological situations with large non-CO_2 effects, indicated by high values and strong gradients of the merged aCCF. In Figure 3 (d) and Figure 4 (d), regions with high gradients at 250 hPa in the merged aCCFs can be found, certainly, these high gradients will provide a high mitigation potential. Thus, e.g. on 15th June 2018, a large mitigation potential can be identified by avoiding warming contrails.

EUROPEAN PARTNERSHIP

Co-funded by the European Union

5 Sensitivity of merged aCCFs to aircraft type

This section will deliver a comprehensive analysis of merged aCCFs. The sensitivity in the merged aCCFs by using emission indices of different aircraft types is shown. The analysis is based on ERA5 reanalysis data.

In the figures of Section 4, we showed the merged aCCFs that assume the metric F-ATR20 (efficacy included) and a transatlantic fleet mean value of the NO_x emission index (EI_{NOx}) and the flown distance per burnt fuel (F_{km}). However, as described in Section 3, there are several choices to generate merged aCCFs. These choices are linked to the emission behaviour of the selected aircraft type and the selected climate metric. In this section, the sensitivity of the merged non-CO_2 aCCFs in relation to different aircraft types is investigated.

5.1 Description of merged aCCF calculations

Table 8 summarizes the technical specification of the merged aCCF calculation. The reference calculation (REF), that was also shown in Section 4, assumes cruise altitude independent transatlantic fleet mean values of EI_{NOx} and F_{km} (detailed values see Section 3). The three sensitivity calculations (SENS-A1, SENS-A2, SENS-A3) assume altitude dependent values of F_{km} and EI_{NOx} for three different aggregated aircraft types (i.e. single-aisle, regional and wide body). They have different values of F_{km} and EI_{NOx} (see Table 3 and Table 4) and, thus, will lead to different merged non-CO_2 aCCFs. Overall, these sensitivity calculations are used to investigate how the aircraft-engine type influences the overall climate impact in terms of average temperature change.

Table 8: Overview of calculated merged non-CO_2 aCCF. Four technical specification of aircraft-engine type selection are possible.

	REF	SENSI-AC1	SENSI-AC2	SENSI-AC3
Metric	F-ATR20	F-ATR20	F-ATR20	F-ATR20
Efficacy	Included	Included	included	included
Aircraft type	Fleet mean values	Single aisle	regional	Wide body

5.2 Analysis of aircraft-engine dependent merged aCCFs

Figure 6 shows the merged aCCFs for REF and for the aircraft dependent sensitivity calculations (SENS-AC1, SENS-AC2 and SENS-AC3) on 15th June, 2018 at a pressure level of 250 hPa. Generally, for all aggregated aircraft types, the highest climate impact is found in the areas of contrail formations. Comparing the aircraft type dependent merged aCCFs reveals that contrails are more dominant for the regional and single-aisle aircraft types. In these cases, the merged aCCFs have very high contrail aCCF values, leading to high absolute merged aCCF values. The maximum merged aCCF values are smaller if the transatlantic fleet mean (REF) and the wide body (SENS-AC3) aircraft type emission indices are chosen. In regions without contrails, the NO_x-induced aCCF (i.e. the sum of the ozone, methane and PMO aCCFs) shows relatively high values for REF and SENS-AC3 compared to those for SENS-AC1 and SENS-AC2. This result is based on the aircraft/engine dependent NO_x emission indices and specific ranges at a flight altitude of 35000 ft, that roughly corresponds to the pressure layer of 250 hPa (Table

EUROPEAN PARTNERSHIP

Co-funded by the European Union

3 and Table 4). Here, the aggregated regional aircraft type shows the lowest EI_{NOx} (7.968), but the highest specific range F_{km} (0.488) of all three aircraft types .

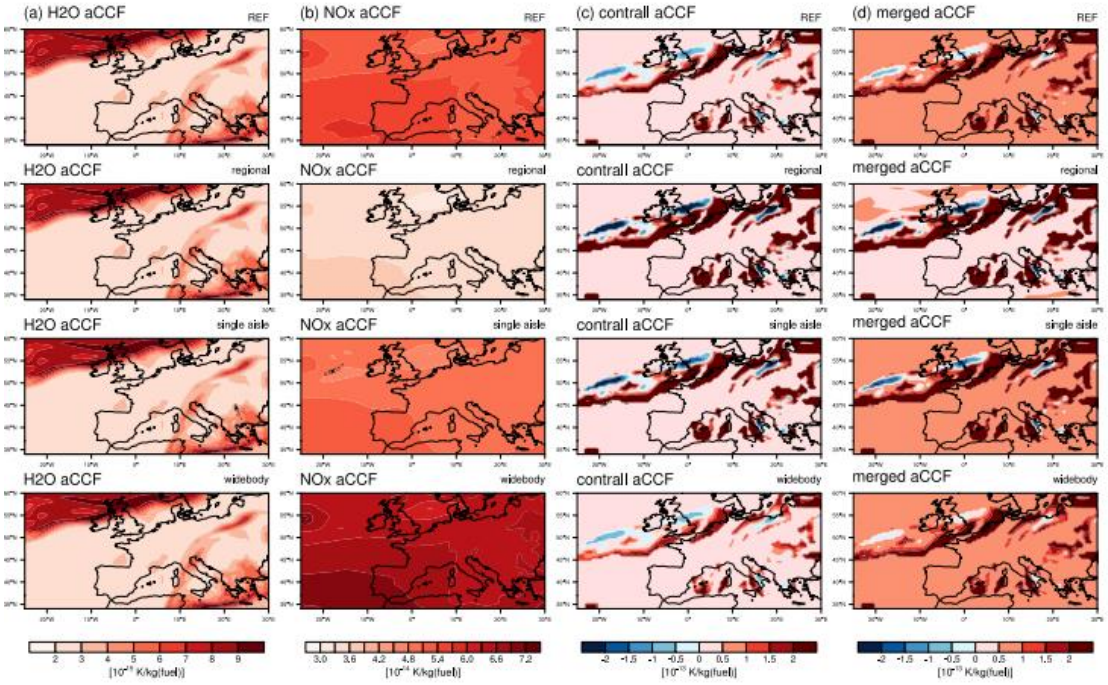

Figure 7: Characteristic patterns of (a) water vapour aCCF [K/kg(fuel)], (b) NO_xaCCF (including O_3, CH_4 and PMO) [K/kg(fuel)] (c) contrail aCCF [K/kg(fuel)], and (d) merged non-CO_2 aCCF [K/kg(fuel)] at pressure level 250 hPa over the European region for 15th June 2018, 12 UTC. Individual and merged non-CO_2 aCCFs are shown for four different assumptions of the NO_x emission index and flown km. For a typical transatlantic fleet, mean (first raw), regional aircraft type (second raw), single aisle aircraft type (third raw) and widebody aircraft type values (forth raw) are given.

EUROPEAN PARTNERSHIP

Co-funded by the European Union

6 Summary and Conclusion

With this deliverable, FlyATM4E presents further developments and expansion of algorithmic climate change functions (aCCFs) as achieved in work package 1 (WP1). Algorithmic climate change functions (aCCFs) represent spatially and temporally resolved information on the climate effects in terms of future temperature changes resulting from aviation emissions at a given time and location in the atmosphere. They include CO_2 and non-CO_2 effects, comprising NO_x, water vapour and contrail-cirrus. These aCCFs can be simply derived from meteorological weather forecast data. Thus they can be used as advanced MET service for climate optimized flight planning in order to inform the airspace users on the climate effect that aviation emission have at a given location. With the help of aCCFs, airspace users can identify those regions of the atmosphere where aviation emission have a large climate effect, e.g. by formation of contrail or ozone. At the same time also information is provided on those regions where aviation emission have a lower non-CO_2 effect, as e.g. no contrail form or NO_x-induced effects are smaller due to atmospheric wash out processes.

Beyond such spatially and temporally resolved quantitative estimates of the climate effect of aviation emissions, it is proposed that such a MET service additionally contains an adequate representation of uncertainties arising from weather forecast and climate science. This advanced MET service provides the basis for robust climate optimzed flight trajectories by providing information on the climate effect of aviation emission and associated uncertainties as an input to expanded flight planning tools, which enables identification of confidence intervalls. Overall aCCFs enable a climate effect assessment of individual aircraft trajectories, using realistic meteorological data along the planned trajectory. Such a climate effect assessment also provides the basis for a climate-optimization of aircraft trajectories and a robustness assessment, as has been shown in the workpackages WP2 and WP3, as reported in the deliverables D2.2 and D3.2.

This deliverable provides a comprehensive description of the prototype algorithmic climate change functions (aCCFs) in Section 2, describing the climate effects of non-CO_2 emissions at a specific location and time for a set of case studies. These aCCFs include aviation's climate effects of water vapour emissions, of NO_x emissions (by triggering ozone formation and methane destruction) and of persistent contrail formation. A consistent set ofaCCFs was developed (aCCF-V1.1) within the FlyATM4E project [Dietmüller]. The aCCFs have been calculated for a set of distinct climate metrics.FlyATM4E also developed a concept of generating merged non-CO_2 aCCFs, which combines individual effects for a given aircraft/engine combination (Section 3). Merged aCCFs can only be constructed with the technical specification of NO_x emission indices and values of flown distance per burnt fuel. Technically, FlyATM4E has developed and published an open-source Python Library, that efficiently calculates both the individual aCCFs and the merged non-CO_2 aCCFs on a daily basis, while using numerical weather prediction data as an input.

Overall, as a result, the FlyATM4E project provides an efficient meteorological (MET) service to inform on the climate effect of flight operations comprising CO_2 and non-CO_2 effects, which represents the solution **Sol-FlyATM4E-01** 'Increased situational awareness on climate change effects relying on algorithmic climate change functions'. The detailed solution text is the following: Having spatially and temporally resolved information on climate effects of aviation emissions in the airspace available is a prerequisite for assessing climate effects of aircraft operations. An efficient integration (in flight planning and airspace management) relies on combining algorithmic climate change functions (aCCFs) with operational numerical weather prediction data of key variables and specific aircraft emissions.This solutions provides information as an efficient meteorological (MET) service to inform on the climate

EUROPEAN PARTNERSHIP

Co-funded by the European Union

effect of flight operations comprising CO_2 and non-CO_2 effects. This solution increases the situational awareness of the airspace user and this climate effect information can be provided as a spatially and temporally resolved data field. The overall climate effect is measured in units of dedicated physical climate metrics. This novel solution developed in FlyATM4E targets to enable assessment and optimization of environmental performance of aircraft operations, more specifically the overall climate effect comprising CO_2 and NO_x-induced, H_2O-induced and contrail cirrus effects [38].

As mathematical calculation of aCCFs includes uncertainties, this deliverable also serves as basis for the assessment of robust climate otimized aircraft trajectories. This advanced concept is applied in work packages 2 and 3 in order to identify climate-optimised aircraft trajectories (Sol-FlyATM4E-02) and to assess the climate impact of ATM operations which integrates an adequate representation of uncertainties. Seasonal and regional analysis of individual aCCFs are provided in Section 4: the characteristic patterns of water vapour, NO_x, contrail and merged aCCFs for specific days over Europe in June and December 2018 at an altitude of 250 hPa are shown. Overall, water vapour and NO_X aCCFs have a warming impact, whereas contrail aCCFs have either a warming or cooling impact during daytime. Merged non-CO_2 aCCFs show a dominant contribution of contrail aCCFs for regions in which contrails are forming. .

It has to be mentioned here that the prototypes of aCCFS which are currently available have been developed for the North Atlantic Flight Corridor, representing summer and winter conditions. For the time being no further updates are available. Hence these algorithms represent a considerable source of uncertainty when aiming for providing detailed quantitative estimates of aviation climate effects and associated mitigation potentials, and further research is required in order to expand the geographic scope and seasonal coverage together with remaining uncertainties of these algorithms.

EUROPEAN PARTNERSHIP

Co-funded by the European Union

7 References

[1] Lee, D. S. et al., 2021: The contribution of global aviation to anthropogenic climate forcing for 2000 to 2018, Atmospheric Environment, 244, doi: 10.1016/j.atmosenv.2020.117834

[2] Frömming, C., Grewe, V., Brinkop, S., Jöckel, P., Haslerud, A., Rosanka, S., van Manen, J. and Matthes, S., 2021: Influence of the actual weather situation on non-CO2 aviation climate effects: The REACT4C Climate Change Functions. Atmospheric Chemistry and Physics, 21(11), 9151-9172

[3] van Manen, J. and Grewe, V., 2019: Algorithmic climate change functions for the use in eco-efficient flight planning. Transportation Research Part D: Transport and Environment,67, 388–405, doi:10.1016/j.trd.2018.12.016

[4] Grewe, V., Frömming, C., Matthes, S., Brinkop, S., Ponater, M., Dietmüller, S., Jöckel, P., Garny, H., Dahlmann, K., Tsati, E., Søvde, O. A., Fuglestvedt, J., Berntsen, T. K., Shine, K. P., Irvine, E. A., Champougny, T., and Hullah, P, 2014: Aircraft routing with minimal climate impact: the REACT4C climate cost function modelling approach V1.0, Geosci. Model Dev., 7, 175-201 10.5194/gmd-7-175-2014

[5] Bauer, P., Thorpe, A. and Brunet, G., 2015: The quiet revolution of numerical weather prediction, Nature, vol. 525, pp. 47—55

[6] Hansen, J.M., Sato, and R. Ruedy, 1997: Radiative forcing and climate response, J. Geophys. Res.,102, 6831-6864, doi:10.1029/96JD03436.

[7] Ponater, M., Marquart, S., Sausen, R. and Schumann, U., 2005: On contrail climate sensitivity, Geophys. Res. Lett., 32, L10706.

[8] Yin, F., Grewe, V., Castino, F., Rao, P., Matthes, S.., Dahlmann, K., Dietmüller, S., Frömming, C., Yamashita, H., Peter, P., Klingaman, E., Shine,K., Lührs, B., Linke, F. 2022: Predicting the climate impact of aviation for en-route emissions: The algorithmic climate change function sub model ACCF 1.0 of EMAC 2.53; GMDD [preprint], https://doi.org/10.5194/gmd-2022-220.

[9] Yamashita, H., Yin, F., Grewe, V., Jöckel, P., Matthes, S., Kern, B., Dahlmann, K., and Frömming, C., 2021: Analysis of aircraft routing strategies for North Atlantic flights by using Airtraf 2.0, Aerospace,8(2), 1–19. doi:10.3390/aerospace8020033

[10] Dietmüller, Matthes, S., Dahlmann, K., Yamashita, H., Soler, M., Simorgh, A., Linke, F., Lührs, B., Meuser, M.M, Weder, C., Castino, F., Yin, F. and Grewe V. 2022: A python library for calculating individual and merged non-CO2 algorithmic climate change functions, GMDD [preprint], https://doi.org/10.5194/gmd-2022-203.

[11] Matthes, S., Dahlmann, K., Dietmüller, S., Yamashita, H., Baumann, S., Grewe, V., Soler, M., Simorgh, A., González Arribas, D., Linke, F., Lührs, B., Meuser, M.M, Castino, F. and Yin, F., 2022: Concept for identifying robust climate-optimized aircraft trajectories in FlyATM4E, in preparation for Applied Science.

[12] FlyATM4E Deliverable D1.1, 2021: Technical note on availability of algorithmic climate change functions (aCCFs) (internal to the FlyATM4E Consortium).

[13]Schumann, U. et al., 2012: A parametric radiative forcing model for contrail cirrus. J. App. Met. Climatol., 51, 1391-1406 10.1175/JAMC-D-11-0242.1

[14]Graver, B. and Rutherford D., 2018: White Paper on Transatlantic Airline Fuel Efficiency Ranking 2017, iCCT – The International Council on Clean Transportation, available at: https://www.theicct.org

[15]Penner et al. 1999: Aviation and the global Atmosphere, Cambridge University Press, UK, 1999

[16]DuBois, D.; Paynter, G. 'Fuel Flow Method 2' for Estimating Aircraft Emissions. SAE Trans. 2006, 115, 1–14.

[17]Jelinek, F, 2004:. Advanced Emission Model (AEM3) v1.5-Validation Report; EEC Report EEC/SEE/2004/004; Eurocontrol: Brussels, Belgium

[18]Nuic, A.; Mouillet, V. *User Manual for the Base of Aircraft Data (BADA) Family 4*; ECC Technical/Scientific Report No. 12/11/22-58; Eurocontrol: Brussels, Belgium, 2012.

[19]Fuglestvedt, J.S. et al., 2010: Transport impacts on atmosphere and climate: Metrics., Atmospheric Environment, 44.37, 4648-4677.

[20]Grewe, V. and Dahlmann, K., 2015: How ambiguous are climate metrics? And are we prepared to assess and compare the climate impact of new air traffic technologies? Atmospheric Environment, 106, 373—374

[21]Dahlmann, K.; Grewe, V.; Frömming, C.; Burkhardt, U., 2016: Can we reliably assess climate mitigation options for air traffic scenarios despite large uncertainties in atmospheric processes? Transp. Res. Part D Transp. Environ., 46, 40–55.

[22]Hansen, J., Sato, M., Ruedy, R., Nazarenko, L., Lacis, A., Schmidt, G., Russell, G., Aleinov, I., Bauer, M., Bauer, S., et al., 2005: Efficacy of climate forcings, Journal of geophysical research: atmospheres, 110

[23]Joshi, M., Shine, K., Ponater, M., and Stuber, N., 2003: A comparison of climate response to different radiative forcings in the general circulation models: toward an improved metric of climate change, Clim. Dyn., 20, 843–854, https://doi.org/10.1007/s00382-003-0305-9

[24]Ponater, M., Marquart, S., Sausen, R., and Schumann, U, 2005.: On contrail climate sensitivity, Geophysical Research Letters, 32

[25]Rap, A., Forster, P. M., Haywood, J. M., Jones, A., and Boucher, O., 2010: Estimating the climate impact of linear contrails using the UK Met Office climate model, Geophysical research letters, 37

[26]Bickel, M., Ponater, M., Bock, L., Burkhardt, U., and Reineke, S., 2020: Estimating the effective radiative forcing of contrail cirrus, Journal of Climate, 33, 1991–2005

[27]Dee, D. P., Uppala, S. M., Simmons, A., Berrisford, P., Poli, P., Kobayashi, S., Andrae, U., Balmaseda, M., Balsamo, G., Bauer, d. P., et al., 2011: The ERA-Interim reanalysis: Configuration and performance of the data assimilation system, Quarterly Journal of the royal meteorological society, 137, 553–597

[28]Irvine, E.A., Hoskins, B.J., Shine, K.P., Lunnon, R.W. and Frömming, C., 2014: A Lagrangian analysis of ice-supersaturated air over the North Atlantic. J. Geophys. Res., 119, 90-100 10.1002/2013JD020251

[29]Rust, H., Richling, A., Bissoli, P. and Ulbrich, U., 2015: Linking teleconnection patterns to European temperature a multiple linear regression mode, Met. Zeitschrift, Vol 24, No. 4, p. 411-423.

[30]Matthes, S. et al., 2021: Mitigation of Non-CO_2 Aviation's Climate Impact by Changing Cruise Altitudes. Aerospace, 8, 36, https://doi.org/10.3390/ aerospace8020036

[31]Yamashita, H., Yin, F., Grewe, V., Jöckel, P., Matthes, S., Kern, B., Dahlmann, K, and Frömming, C., 2020: Newly developed aircraft routing options for air traffic simulation in the chemistry–climate model EMAC 2.53: AirTraf 2.0. Geoscientific Model Development, 13 (10), 4869–4890. doi: 10.5194/gmd-13-4869-2020

[32]Rosanka, S., Frömming, C., and Grewe, V., 2020: The impact of weather patterns and related transport processes on aviation's contribution to ozone and methane concentrations from NO_x emissions, Atmos. Chem. Phys., 20, 12347–12361

[33]FlyATM4E Deliverable D3.2, 2022: Report on final results on eco-efficient trajectories

[34]FlyATM4E Deliverable D2.2,2022: Report on results andassessments of the robustness of eco-efficient trajectories

[35]González-Arribas, D., Andrés-Enderiz, E., Soler, M., Jardines, A., & Garcıa-Heras, J. Probabilistic 4D Flight Planning in Structured Airspaces through Parallelized Simulation on GPUs. In: International Conference for Research in Air Transportation (ICRAT) 2020.

[36]Jöckel, P. et al., 2010: Development cycle 2 of the Modular Earth Submodel System (MESSy2). Geoscientific Model Development, 3 (2), 717–752. doi: 10.5194/gmd-3-717-2010

[37]Lührs, B., Linke, F., Matthes, S., Grewe, V., and Yin, F.: Climate impact mitigation potential of European air traffic in a weather situation with strong contrail formation, Aerospace, 8, 50, 2021.

[38]FlyATM4E Deliverable D5.3, 2022: Final Project Results Report.

Appendix A Mathematical formulation of aCCFs

Here we present the mathematical formulas of the aCCFs, which describe the climate impact as a five-dimensional data set (latitude, longitude, altitude, time, type of emission). Simple statistical methods were used to derive aCCFs. A detailed explanation of the aCCFs approach can be found in [3] for NO_x induced species and water vapour, and in the case of the contrail aCCFs approach, a detailed description is given in [9][8]. In the following, we describe the mathematical formulation of all the individual aCCFs. All aCCFs are consistently given in ATR20 using pulse emission and without taking efficacy into account.

A.1 NO_x induced aCCFs

The total NO_x aCCFs is a combined effect of the NO_x induced ozone aCCFs and the NO_x induced methane aCCFs. This can be explained by the fact that the NO_x emissions of aviation led to the formation of ozone (O_3) which induces a warming of the atmosphere. Additionally, NO_x emissions lead to the destruction of the long lived GHG methane (CH_4) which then induces a cooling of the atmosphere. In the following, the mathematical formulation of both the ozone and the methane aCCFs is described.

A.2 Ozone aCCFs

The mathematical formulation for the ozone aCCFs is based on temperature T [K] and geopotential Φ [m^2/s^2]. The relation for the ozone aCCFs ($aCCF_{O3}$) at a specific atmospheric location and time is given in temperature change per emitted NO_2 emission [K/kg(NO_2)]:

$$aCCF_{O3} = \begin{cases} aCCF'(T,\Phi) \\ 0 \end{cases} \text{ for } \begin{matrix} aCCF\prime>0 \\ aCCF\prime\leq 0 \end{matrix}$$

with $aCCF'(T,\Phi) = -5.20 * 10^{-11} + 2.30 * 10^{-13} * T + 4.85 * 10^{-16} * \Phi - 2.04 * 10^{-18} * T * \Phi$

Accordingly, the ozone aCCFs takes positive values, and is set to 0 in case of negative aCCF' values.

A.3 Methane aCCFs

The methane aCCFs is based on the geopotential Φ [m^2/s^2] and the incoming solar radiation at the top of the atmosphere F_{in} [W/m^2]. The relation of the methane aCCFs ($aCCF_{CH4}$) at a specific location and time is given in temperature change per emitted NO_2 emission[K/kg(NO_2)]:

$$aCCF_{CH_4}(\Phi, F_{in}) = \begin{cases} aCCF'(\Phi,F_{in}) \\ 0 \end{cases} \text{ for } \begin{matrix} aCCF'(\Phi,F_{in})<0 \\ aCCF'(\Phi,F_{in})\geq 0 \end{matrix}$$

with $aCCF'(\Phi, F_{in}) = -9.83 * 10^{-13} + 1.99 * 10^{-18} * \Phi - 6.32 * 10^{-16} * F_{in} + 6.12 * 10^{-21} * \Phi * F_{in}$

Thus, the methane aCCFs is negatively defined. It is set to 0 if the term aCCF' is 0 or positive.

F_{in} is defined as incoming solar radiation at the top of the atmosphere as a maximum value over all longitudes and is calculated by: $F_{in} = S * cos\theta$, with total solar irradiance S=1360 Wm^{-2} , with $cos\theta = \sin(\varphi)\sin(d) + \cos(\varphi)\cos(d)$ and with d = -23.44° cos(360°/365 * (N + 10)). Here θ is the solar zenith angle, ϕ is latitude, and d is the declination angle, which defines the time of year via the day of the year N.

The mathematical formulation of the ozone aCCF is only valid for the short-term ozone effect of NO_x. The primary mode ozone (PMO), which describes the long-term decrease in the background ozone, as result of a methane decrease, is not included [3] . Thus if merging total NO_x effect be aware that only

EUROPEAN PARTNERSHIP

Co-funded by the European Union

the NO_x effect on short term ozone increase and on methane decrease is taken into account. For NO_x induced PMO climate impact we have the possibility to include it to the total NO_x aCCF, as the PMO aCCF can be derived by applying a constant factor of 0.29 to the methane aCCF [21].

A.4 Water vapour aCCFs

The water vapour aCCFs is based on the Potential Vorticity (PV) given in standard PV units $[10^{-6}\mathrm{K\,kg^{-1}\,m^2\,s^{-1}}]$. The following the relation of the water vapour aCCFs ($aCCF_{H20}$) at a specific location and time is given in temperature change per fuel [K/kg(fuel)]:

$$aCCF_{H_2O}(PV) = 4.05 * 10^{-16} + 1.48 * 10^{-16} * |PV|$$

The absolute value is the PV is taken to enable a calculation on the southern hemisphere, where PV has a negative sign.

A.5 Contrail aCCFs

The aCCFs of persistent contrail cirrus have been developed within the EU project ATM4E. A detailed description and verification of these contrail aCCFs are under[8]. The algorithm that generates contrail aCCFs is obtained by the calculation of the contrail radiative forcing, using ERA-Interim data as input. In contrast, the above described NO_x and H_2O aCCFs are based on CCFs that were calculated with the chemistry climate model EMAC.

Contrail aCCFs are calculated separately for day-time and night-time contrails, because their climate impact differs between daylight and darkness, as the shortwave forcing is only relevant for daylight conditions. To differ between day-time and night-time contrail aCCFs, the local time and solar zenith angle are calculated. For locations in darkness, the time of sunrise is calculated. If the time between the local time and sunrise is greater than 6 h, the night-time contrail aCCFs is applied. In order to determine the contrail aCCFs, the RF of day-time or night-time contrails is calculated as described in the following.

The **RF of day-time contrails** ($\mathrm{RF_{aCCF-day}}$) in $[\mathrm{W/m^2}]$ is based on the outgoing longwave radiation (OLR) in $[\mathrm{W/m^2}]$ both at the time and location of the contrail formation. For a specific atmospheric location and time, the $\mathrm{RF_{aCCF-day}}$ is given by:

$$RF_{aCCF-day}(OLR) = 10^{-10} * (-1.7 - 0.0088 * OLR)$$

According to the equation, the RF for the daytime contrails can take positive and negative values, depending on the OLR.

The **RF of night-time contrails** ($\mathrm{RF_{aCCF-night}}$) in $[\mathrm{W/m^2}]$ is based on temperature (T) in [K]. For an atmospheric location $(\mathrm{x, y, z})$ at time t:

$$RF_{aCCF-night} = \begin{cases} RF_{aCCF-night}(T) = 10^{-10} * \left(0.0073 \times 10^{0.0107 * T} - 1.03\right) & \text{for } \overset{T > 201K}{else} \\ 0 \end{cases}$$

For temperatures less than 201 K, the night-time contrail is set to zero.

The above calculated RF of contrails can be converted to global temperature change (ATR20) by just multiplying with a constant factor of 0.0151 K/(W/m2) (Dahlmann, pers. Communication, 10/2021). The resulting contrail aCCFs are then given in temperature change per flown kilometre [K/km(contrails)].

EUROPEAN PARTNERSHIP

Co-funded by the European Union

Of course, contrail aCCFs are only relevant at locations where persistent contrails can form and accordingly regions without persistent contrails have to be set to zero. In climate simulations (as, e.g., EMAC), there is the possibility to calculate the potential contrail coverage at each timestep, and thus it can be taken to mask regions where contrails do not form permanently. If the potential contrail cover is not available as an input variable, e.g., in the weather forecast or reanalysis data, locations in which persistent contrails can form, are identified by two conditions: temperature below 235 K and relative humidity with respect to ice at or above 100 %. Alternatively, the more accurate Schmidt-Appleman-criterion, which additionally considers the aircraft engine type, could be used

A.6 CO_2 aCCF

In order to compare these merged non-CO_2 aCCFs to the climate impact of CO2 a value for a CO_2 aCCFs is calculated with the climate-chemistry response model AirClim [21]. In case of the pulse scenario used also for the aCCFs above, the CO_2 is given by $6.94*10^{-16}$[K/kg(fuel)] (K. Dahlmann, personal communication, 2021). Note, however, that the CO_2 aCCFs highly varies with the used emission scenario

EUROPEAN PARTNERSHIP

Co-funded by the European Union

Appendix B Additional figures

B.1 Synoptic situation for selected days

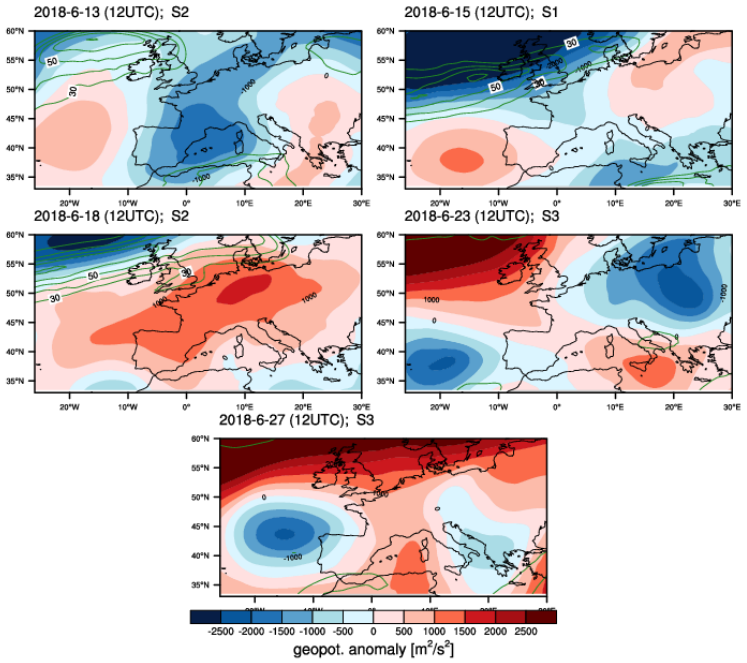

Figure B1: Daily mean geopotential anomaly (in m^2/s^2) at pressure level 250 hPa over European region for 5 selected days in June 2018.

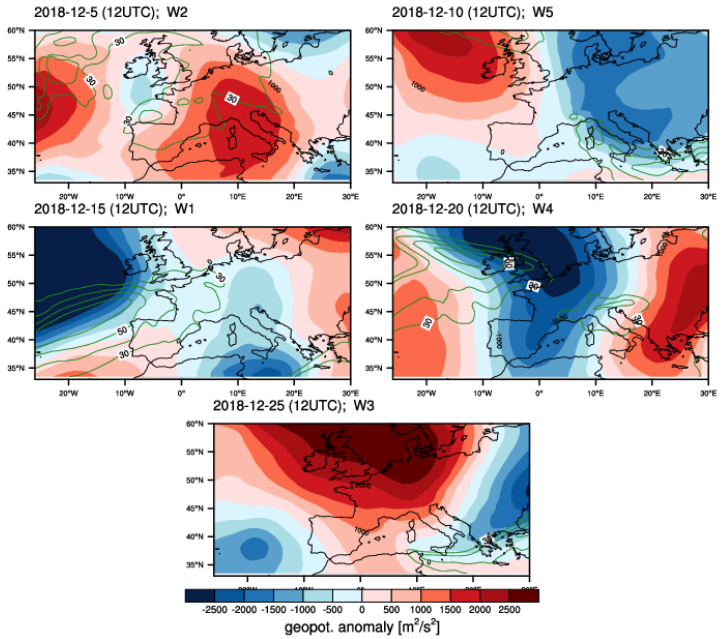

Figure B2: Daily mean geopotential anomaly (in m^2/s^2) at pressure level 250 hPa over European region for 5 selected days in December 2018.

Co-funded by the European Union

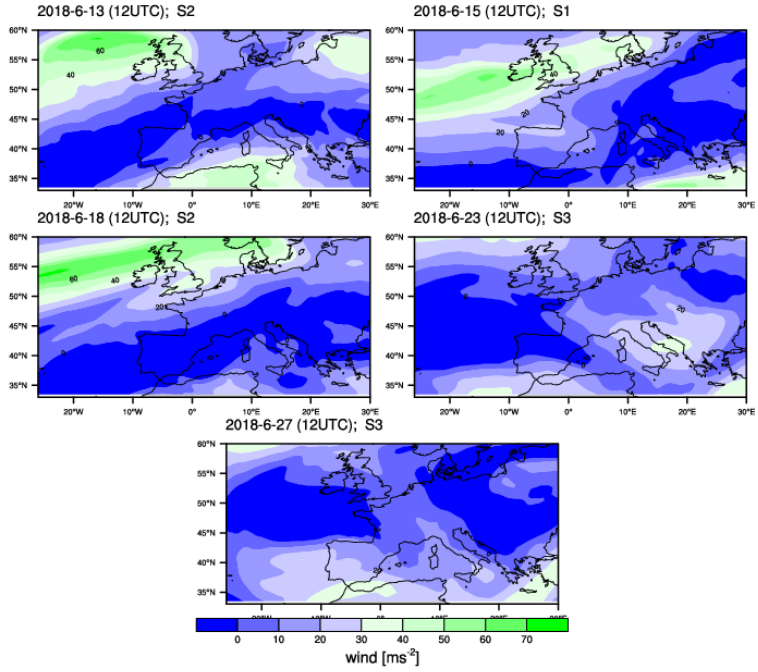

Figure B3: Zonal wind speed (in m/s^2) at pressure level 250 hPa over European region for 5 selected days in June 2018.

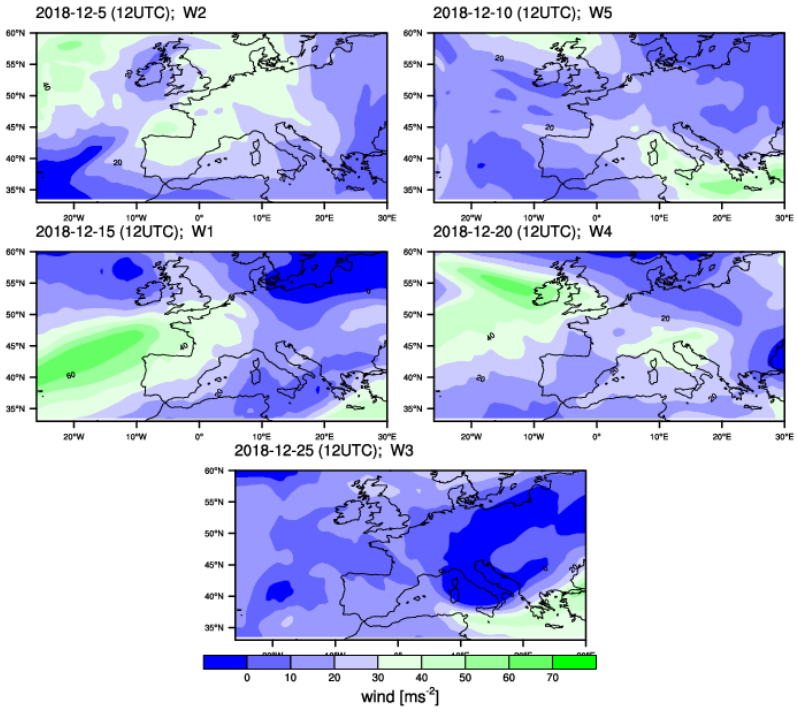

Figure B4: Zonal wind speed (in m/s^2) at pressure level 250 hPa over European region for 5 selected days in December 2018.

Co-funded by the European Union

B.2 Weather pattern classification

To investigate the influence of synoptic weather patterns on the climate impact of aviation daily weather patterns over the North Atlantic have been classified into five typical patterns in winter and three typical patterns in summer in the EU project REACT4C [1]These patterns were characterized by the two teleconnection patterns North Atlantic Oscillation (NOA) and East Atlantic (EA) and by the strength and position of the jet stream (see Table B1).

Table B1: Characterization of North Atlantic weather types for winter (referred to as W1-W5) and summer (referred to as S1-S3) and their resulting characteristic weather pattern over Europe. This table is adopted from [12] and refers to the classification of [28].

Weather Type	NOA/EA index	jet stream position/strength	selected characteristics for European weather patterns
W1	EA+	Zonal/strong	Low pressure Atlantic and NW-Europe, strong northern jet
W2	NAO+	Tilted/strong	High pressure SW-Europe, strong northern jet
W3	EA-	Tilted/weak	High pressure northern Europe, northward shifted jet
W4	NAO-	Confined/strong	Low pressure Europe, high pressure north of 60°N, southward shift of jet
W5	mixed	Confined/weak	W5 highly variable over Europe
S1	EA+	Zonal/strong	Low pressure over Atlantic and northern Europe, strong jet
S2	mixed	Weakly tilted/weak	Low pressure northern Atlantic, high pressure SW-Europe
S3	EA-	Strongly tilted/weak	High pressure Atlantic and western Europe, low pressure over eastern Europe, northward shifted jet

As the European region is also highly influenced by the North Atlantic teleconnection patterns (see e.g.[28]), we use these weather types as a first approximation to characterize the European weather situation. The typical synoptic weather types over the North-Atlantic (i.e. W1-W5 and S1-S3, as characterized in[28]) and the weather patterns over Europe which are linked to these North-Atlantic weather types are given in Table B1.

EUROPEAN PARTNERSHIP

Co-funded by the European Union

B.3 Analysis of night time aCCFs

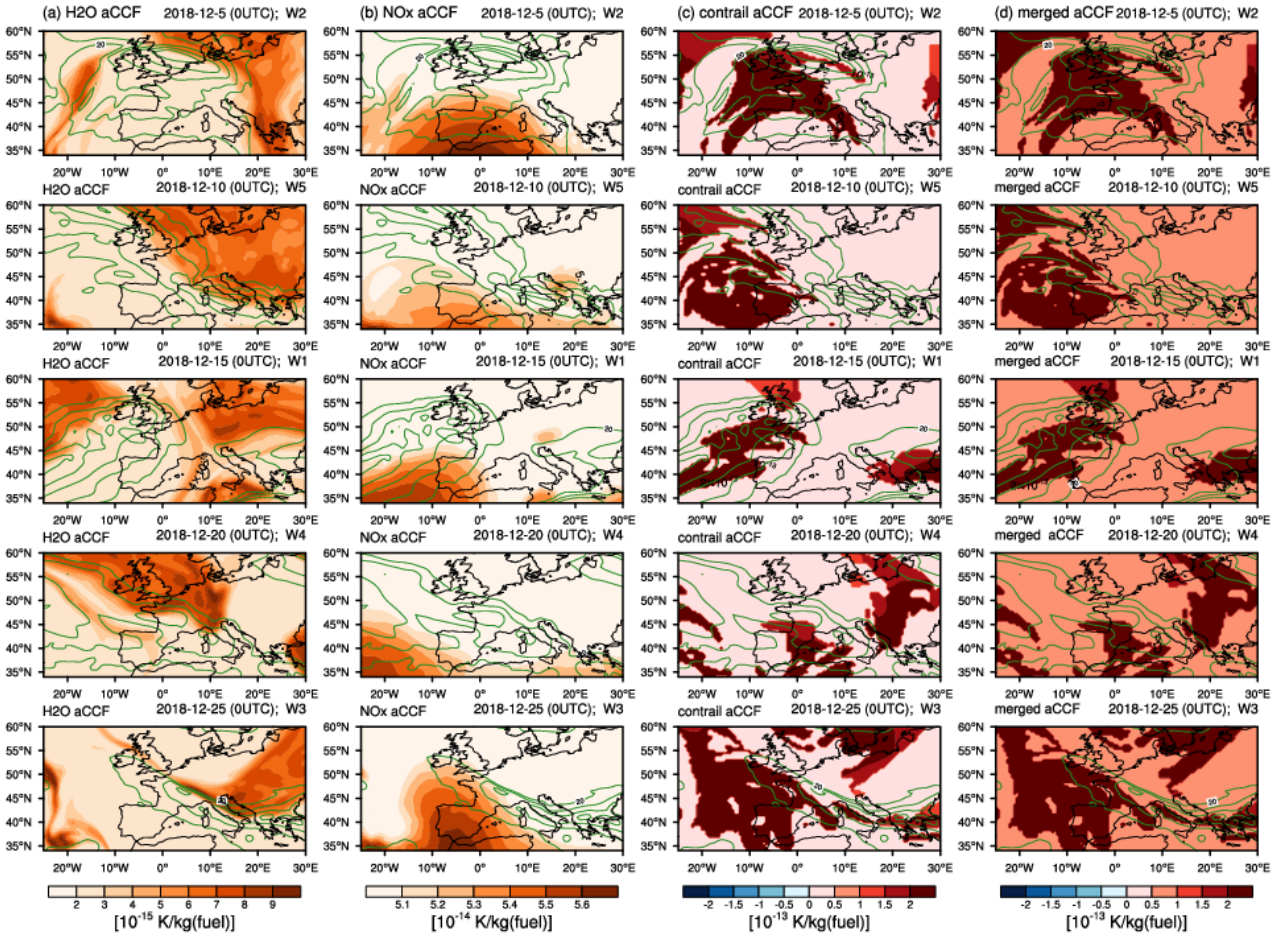

Figure B5: Characteristic patterns of aCCF (a) water vapour aCCF [K/kg($_{fuel}$)] (b) NO_xaCCF (including O3, CH4 and PMO) [K/kg(fuel)] (c) contrail (nighttime) aCCF [K/kg(fuel)] (d) merged non-CO_2 aCCF [K/kg(fuel)] at pressure level 250 hPa over European region for 5 selected days in December 2018, at 0UTC. Individual aCCFs were calculated from ERA5 reanalysis data. Overlaid green lines indicate wind spreads over 30 m/s$^{2.}$ Moreover the weather situation of the specific days was classified according to [12] and is given right beside the date).

EUROPEAN PARTNERSHIP

Co-funded by the European Union

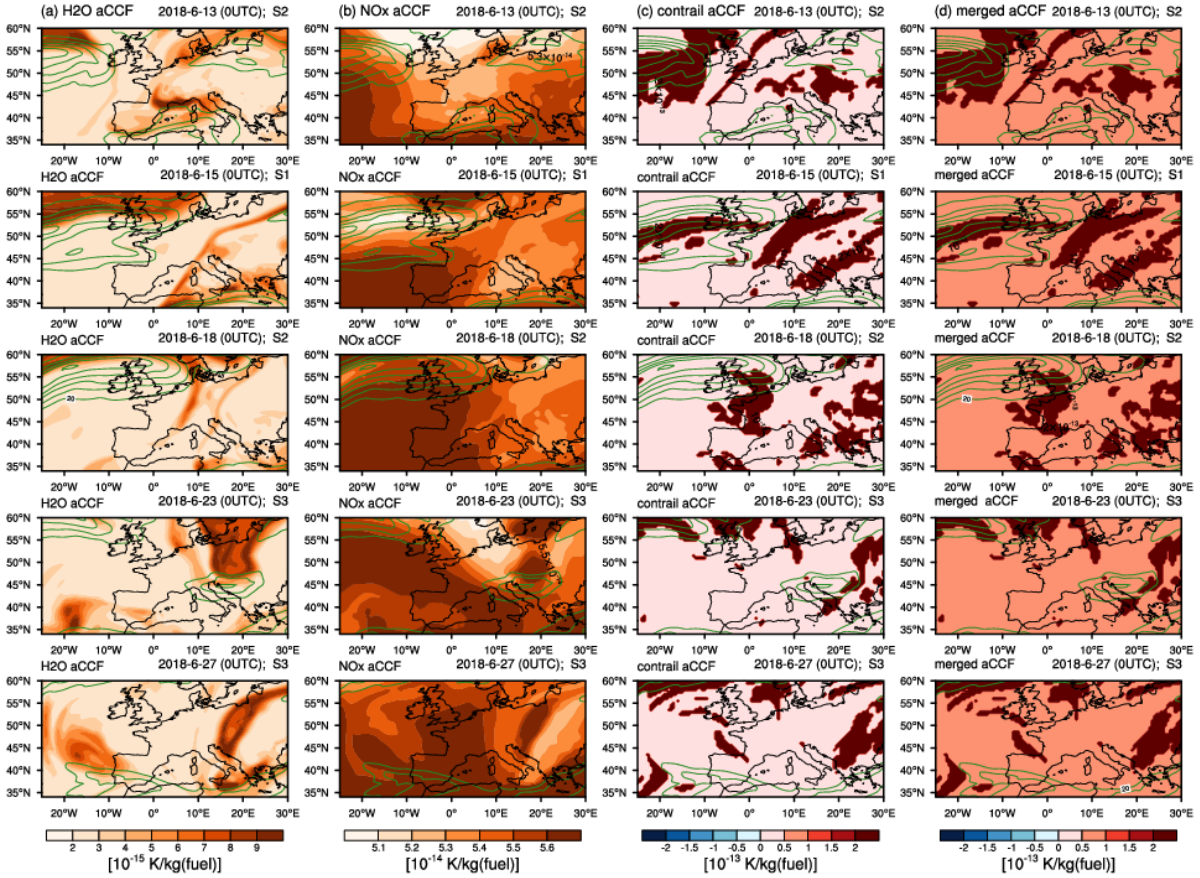

Figure B6: Characteristic patterns of aCCF (a) water vapour aCCF [K/kg($_{fuel}$)] (b) NO_xaCCF (including O3, CH4 and PMO) [K/kg(fuel)] (c) contrail (nighttime) aCCF [K/kg(fuel)] (d) merged non-CO_2 aCCF [K/kg(fuel)] at pressure level 250 hPa over European region for 5 selected days in June 2018, at 0UTC. Individual aCCFs were calculated from ERA5 reanalysis data. Overlaid green lines indicate wind spreads over 30 m/s^{2,} (Moreover the weather situation of the specific days was classified according to [12] and is given right beside the date).

EUROPEAN PARTNERSHIP

Co-funded by the European Union

B.4 Vertical profile of aCCFs

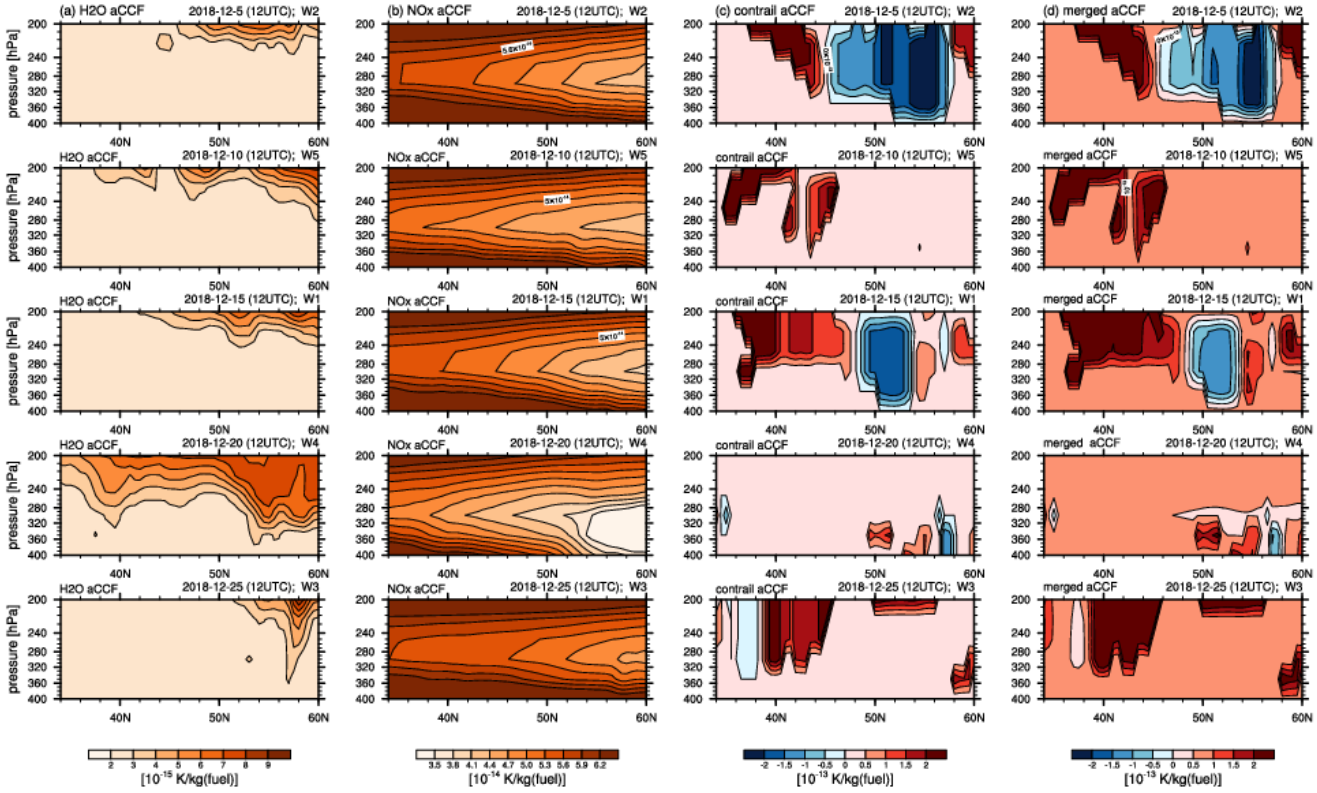

Figure B7 . Vertical cross section patterns of aCCF (a) water vapour aCCF [K/kg($_{fuel}$)] (b) NO_xaCCF (including O3, CH4 and PMO) [K/kg(fuel)] (c) contrail (daytime) aCCF [K/kg(fuel)] (d) merged non-CO_2 aCCF [K/kg(fuel)] at longitude 0° for 5 selected days in December 2018, at 12UTC. Individual aCCFs were calculated from ERA5

EUROPEAN PARTNERSHIP
Co-funded by the European Union

Acronyms and FlyATM4E consortium

Table 9: Non-exhaustive list of acronyms used across the text.

Acronym	Description
aCCF	algorithmic climate change functions
AirTraf	Air Traffic simulator
ATM	Air Traffic Management
ATS	Air Traffic Services
ATR20	Average temperature response over 20 years
BAU	business as usual
CCF	Climate change functions
ECMWF	European Centre for Medium-Range Weather Forecasts
EMAC	ECHAM5/MESSy2 Atmospheric Chemistry Model
EA	East Atlantic
EPS	Ensemble Prediction System
EI	Emission index
EI_{NOX}	nitrogen emission index
CLIMaCCF	Environmental Library
ERA-5	5^{th} generation of ECWMF reanalysis
ERF	Effective radiative forcing
EU	European Union
F_{km}	Flown distance per burnt fuel
GHG	Greenhouse gas
H_2O	Water vapour
PV	Potential Vorticity
PMO	Primary Mode ozone
ISSR	ice supersaturated regions
NAFC	North Atlantic flight corridor
NAO	North Atlantic Oscillation
R-aCCF	Robust aCCF
NO_x	Nitrogen oxide
RF	Radiative forcing
ROOST	robust optimization of structured trajectories
SESAR	Single European Sky ATM Research Programme

EUROPEAN PARTNERSHIP

Co-funded by the European Union

SJU	SESAR Joint Undertaking
TOM	trajectory optimization module
WP	Work Package

Table 10: FlyATM4E consortium acronyms

Acronym	Description
DLR	DEUTSCHES ZENTRUM FUER LUFT - UND RAUMFAHRT EV
TUD	TECHNISCHE UNIVERSITEIT DELFT
TUHH	TECHNISCHE UNIVERSITAT HAMBURG
UC3M	UNIVERSIDAD CARLOS III DE MADRID

EUROPEAN PARTNERSHIP

Co-funded by the European Union

Co-funded by the European Union